Valorisation of Used Automotive Lubrication Oil

Tegan Van Zyl

Dissertation submitted for the fulfilment of the requirements for the degree Master of Engineering in the Department of Chemical Engineering at Durban University of Technology

Thesis Supervisor: S. Rathilal

Y.M. Isa

Department of Chemical Engineering

Durban University of Technology

January 2019

Declaration

I understand the meaning of plagiarism and in knowing, declare the work contained in this thesis, save for that which is properly acknowledged, to be my own.

Signed [redacted]

Date : 27/01/2019

‘The only thing that interferes with my learning is my education.’

Albert Einstein

Acknowledgements

To my family, the first thanks goes to you for all your support and encouragement throughout my academic career and especially during this dissertation. To my Supervisor Prof S. Rathilal, thank you for all your advice, assistance and patience. Thank you to my colleagues Ntuthuko and Keshnee for all of your assistance, Ntuthuko for your help with building the pilot plant and Keshnee for your help in the lab.

Abstract

This study has explored the production of Light Oil 10 (LO10) fuel from used automotive lubrication oil, thus providing a method for producing a cheaper alternative to diesel and paraffin for the South African industrial heating fuel market. Used automotive lubrication oil has different physical properties to that of the specified properties for Light Oil 10 fuel and therefore has to undergo processing that aligns the properties of the two.

The low availability of Light Oil 10 fuel in the South African industrial heating market is driving companies such as a Durban based oil refinery to develop a continuous process that will produce Light Oil 10 fuels without the supplementation of paraffin. The supplementation has been done to retain customers but this resulted in the company selling Light Oil 10 fuel at a loss.

Used automotive lubrication oil was of particular interest for use as the raw material for the new process as it is of low cost and is readily available. The viscosity (a measure of how easily a fluid flows at a particular temperature) of used lubrication oil was too high and needed to be reduced before it could qualify as Light Oil 10. The reduction of the viscosity of a fluid means that the ability of the fluid to flow at a particular temperature has improved. Additionally the additive package and the impurity content of the used automotive oil were too high. The additive package is added to mineral oil to give it the properties that new automotive lubrication oil requires; this package is still present in used automotive lubrication oil and is responsible for the high level of impurity content because it prevents impurities from agglomerating and dropping out of the oil. The new process was therefore required to be able to reduce the viscosity of used automotive lubrication oil and break the additive package.

The required process and operating variables were developed / identified through literature review (qualitative) and the optimum operating variables were identified through experimentation (quantitative). A design of experiment was carried out using Design Expert software. This identified the matrix of runs that were required in identifying the optimum temperature, pressure and residence time for the ranges specified. The product from each of the runs was analysed in the Durban based oil refinery Research and Development lab. The results from the lab along with the corresponding run conditions were used to develop a model, and the model used to identify the optimum operating conditions. The research and experimentation took a total of two years to complete.

The literature review found an existing refinery process, the drum type visbreaker to be the most suitable process for reducing the viscosity and breaking the additive package of used automotive lubrication oil. The drum type visbreaker holds oil in the drum for a period of time known as the residence time, at temperatures and pressures of 443^{o}C and 15 bar respectively. These three variables are the critical operating variables in the visbreaking process. The high temperature breaks the large molecules into smaller molecules thereby reducing the viscosity via a process known as thermal cracking. This process also breaks down the additive package.

The results from the experimental runs revealed that it is possible to produce Light Oil 10 from used automotive lubrication oil using the drum type visbreaker. The model produced through experimentation was found to be reliable and accurate within the range of variables investigated at predicting results for future runs. The model was also successfully used to identify the optimum operating conditions at which Light Oil 10 is produced from used automotive lubrication oil. The conditions were found to be 475^{o}C, 15 bar and 60 minutes, confirmed by three confirmation runs.

In conclusion this study has identified through literature and experimentation that thermal cracking via the free radical mechanism is the preferred process for producing Light Oil 10 from used automotive lubrication oil at liquid yields greater than 90%. An appropriate model was generated using the critical operating variables to predict future viscosity results.

It was recommended that the Durban based oil refinery design and build a production scale pilot plant that includes all equipment and the feed heating coil (furnace used to heat feed to 475^{o}C) that a full scale plant would have. This is because the run lengths due to coking (build up of hard carbon on the surfaces of heat exchange equipment) and functionality of the process need to be confirmed before the process can be deemed to be economically viable. Once this has been achieved a full scale production facility can be built.

Contents Page

List of Tables

List of Figures

Nomenclature

υ : Viscosity @ 40^{o}C in cSt

T : Temperature in degrees Celcius

P : Pressure in bar (gauge)

τ : Residence time in minutes

List of Abbreviations

APO : Asphaltene precipitation onset

API : American petroleum institute

ARDO : Asphaltene resin-deposition onset

ARFO : Asphaltene resin-flocculation onset

B.D.E : Bond dissociation energy

DBSA : 4-Dodecylbenzenesulfonic acid

DOE : Design of experiment

FCC : Fluidised catalytic cracker

FFS : Fuel firing systems

GHU : The Genoil Hydroconversion process

HCAT : The Catalytic heavy oil upgrading process

HDM : Hydro-de metallisation

HDN : Hydro-denitrogenation

HDS : Hydro-desulphurisation

HTL : The Heavy to Light upgrading process

LO10 : Light Oil with a viscosity of 10cSt at 40 degree Celsius

LPG : Liquified petroleum gas

PBC : Pre-baked clay

PISRHM : The Process for Intensive Separation of Raw Hydrocarbon Material

SCC : Steam catalytic cracking

TOC : Thermal oxidative cracking

UALO : Used automotive lubrication oil

VTB : Vacuum tower bottoms

1 Introduction

The manufacturing of industrial heating fuels is essential for the success of industry in South Africa as they are cheaper than diesel, paraffin, LPG and petrol. Industrial heating fuels are used in boilers to make steam used to generate electricity, in furnaces to make bricks and various other products that require curing, in ovens to bake bread and in incinerators to burn hazardous waste.

Depending on the type, application and location of the specific industry, the fuel quality and hence the fuel price varies by a large amount. Industries in urban areas have strict limits on their air emissions and therefore have to burn cleaner fuels that contain low levels of sulphur and metals. These urban industries also require an easy burning fuel with a low viscosity. Such a fuel does not require heating in order to achieve the required atomisation in the combustion chamber. Effective atomisation improves the air/fuel mixture and promotes complete combustion. Heating requires additional equipment, consuming additional energy and increasing odour emissions.

Industries that utilise boilers and ovens that can be damaged by the build up of ash on heat transfer surfaces require cleaner fuels that contain low levels of metals. All these industries require a fuel with the physical properties of diesel and paraffin but at a lower price.

LO10 is a low cost alternative to paraffin and diesel. LO10 is not readily available and it is this shortage in supply of LO10 to the industrial heating fuel market that is driving a Durban based oil refinery to develop a continuous process that will produce LO10 without the supplementation of paraffin. The supplementation is done to retain customers and in doing so the Durban based oil refinery is selling LO10 at a loss.

Used automotive lubrication oil (UALO) is of particular interest for use as the raw material as it is of low cost and readily available. However, the viscosity, ash, sediment, soot and impurity content of UALO is too high and must first be reduced before it can qualify as LO10. UALO also contains additives. These additives add to the ash content and keep impurities/ash/sediment/additives in suspension preventing their removal. The developed process will have to be capable of removing these additives and significantly reduce the viscosity of the UALO at acceptable yields.

This research aimed to provide a suitable process for the production of LO10 from UALO.

1.1 Scope

The research aimed to develop/identify the most efficient process that, from UALO, will produce a low viscosity, low ash and low sediment alternative to diesel and paraffin. Important operating variables of the selected process were identified and optimised in order to achieve the sufficiently high yields and required specifications of LO10.

1.2 Research Objectives

The main aim of this project is to identify a method to produce LO10 from UALO at a yield greater than 90%.

In order to achieve this aim the following objectives were required to be met

1.2.1 Identify a suitable process

The following questions need answers in order to satisfy the above objective

a. What existing oil refinery processes will reduce the viscosity of used automotive lubrication oil?

b. How to breakdown the additive package found in used automotive lubrication oil?

c. What are the critical operating variables for the identified suitable process?

d. How do these variables affect the viscosity, yield and additive package?

1.2.2 Design a bench top test rig

The following questions need answers in order to design the bench top test rig.

a. What is the layout of the plant?

b. What are the required materials for construction?

c. What is the required control philosophy?

1.2.3 Build the designed bench top test rig

1.2.4 Conduct a design of experiment (DOE)

The following questions need to be answered in order to carry out the DOE

a. Number of input variables?

b. What are the ranges of the input variables

c. How many response variables

d. What is the study type?

e. What is the design type?

1.2.5 Perform said trials on bench top test rig

1.2.6 Develop a model and use it to identify the optimum operating conditions

1.2.7 Draw a conclusion to the findings

The research paradigm is both qualitative and quantitative. Qualitative in that a process will be identified through research and quantitative in that experimentation will be carried out on the process in order to identify the optimum operating variables.

1.3 Thesis structure

The thesis is structured as follows:

The literature review in Chapter 2 sets out to give a greater understanding of where UALO comes from, its physical and chemical properties and the problems associated with converting it to LO10. Ultimately this reveals the list of questions that need to be answered in order to achieve the objectives of this thesis. The review explains how these questions are answered.

In Chapter 3 the methodology used in this thesis is discussed and the process in which the research questions were answered is justified.

Chapter 4 presents the results of all research undertaken. The results are critically analysed and discussed in terms of the research questions asked.

Chapter 5 draws conclusions from the discussion and presents recommendations to the Durban based oil refinery.

2 Literature Review

2.1 Background

The current lack in supply of low viscosity oil (LO10) to the industrial heating fuel market is driving research into alternative methods of producing the low cost alternative to paraffin and diesel. UALO is of particular interest for use as the raw material, as it is of low cost and readily available. However the viscosity, ash, sediment, soot and impurity content of UALO is too high, and must first be reduced before it can qualify as LO10. Some specifications must be met before UALO can be considered LO10. Refer to chapter three for UALO properties and LO10 specifications.

One of the most important specifications of LO10 is the viscosity. In order to determine the process required to achieve LO10 specifications (refer to Chapter 3 for specifications); one requires a greater understanding of the source and properties of the UALO.

2.2 Used Automotive Lubrication Oil

Lubrication oil manufactured for use in internal combustion engines consists of refined mineral oil and an additive package. This additive package contains additives such as friction modifiers, anti-wear agents, anti-oxidant additives, anti foam agents, detergents, viscosity modifiers and pour point depressants. Friction modifiers are added to reduce friction and therefore engine wear. They adsorb onto the surfaces of the engine forming thin lubricant films. Long chain fatty acids and molybdenum compounds make up the friction modifiers. The long chain fatty acids double as surfactants keeping unwanted products of combustion in suspension. Anti-wear agents are added to reduce wear and are composed of organo-sulfur and organo-phosphorus compounds. Antioxidant agents are added to prolong the service life of the lubrication oil by preventing/delaying the oxidation of the oil in engines. The following compounds are used as antioxidants (Ahmed and Nassar, 2011):

- Sulfur compounds
- Phosphorus compounds
- Aromatic amine compounds
- Organo-alkaline earth salt compounds
- Organo-metallic compounds

Corrosion inhibitors are added to form protective films on the engine surfaces preventing water from reaching them. They consist of amine succinates and alkaline earth sulfonates. Detergent and dispersant additives are added to suspend undesirable products of combustion and oxidation, preventing them from being deposited on engine surfaces. Viscosity index improvers/ modifiers are high molecular weight polymers and are added to increase the relative viscosity of lubricating oils more at higher temperatures than at lower ones. Pour point depressants such as alkylaromatic polymers are added to prevent wax crystals from adhering to each other at low temperatures and preventing flow (Ahmed & Nassar, 2011).

UALO is generated in internal combustion engines. This waste oil has high values of ash, carbon residue, asphaltenes, metals, water, resin, varnish, lacquer and other unwanted materials. The sources of these include (but are not limited to the additive package discussed above), oxidation and thermal degradation (Abdel-Jabbar, Zubaidy & Mehrvar, 2010).

The additives contribute to the high ash and sediment content because they both contain metals and keep unwanted ash and sediment in suspension. The interaction between asphaltene clusters and the presence of the viscosity modifier both contribute towards the viscosity of lube oil (Badger & Harold, 2001). It is therefore desired that the additives be removed to allow for sedimentation/filtration and viscosity reduction.

2.3 Asphaltenes

Asphaltenes are also found in petroleum and consist of a dispersion of very small platelets (3.5 nanometres) that easily pass through pore passages. These platelets are created by compounds (maltenes and resins) that form micelles. Micelles are formed by chemicals known as surfactants. Surfactants are polar molecules. The non-polar end is hydrophobic and the polar end is hydrophilic (Shaw, 1992). The hydrophilic heads attach themselves to the asphaltene particle, and the hydrophobic head attracts a film of oil preventing the asphaltenes from agglomerating and dropping out. When the micelles are stable, asphaltene particles remain in suspension and are not a significant problem in oil. However, when these micelles are broken by chemical or physical (high temperature) interactions, the asphaltene particles agglomerate and drop out creating extremely viscous sludge in the oil.

Asphaltenes have a large molecular weight and contain high levels of metals. In thermal cracking, asphaltenes remain unaffected while additional asphaltenes can be formed by secondary polymerisation reactions (Sieli, 1998). Grouping of asphaltenes at temperatures above 400^{o}C leads to cross linking and dehydration, yielding coke particles with a radius of

1-5 μm. Grouping at lower temperatures result in precipitation and fouling of furnaces and heat exchangers (Agorreta et al., 2011). They are more likely to precipitate in oils that have a high viscosity and density. The resulting sludge is insoluble in pentane, kerosene and diesel, and only slightly soluble in aromatic solvents such as xylene. They have a preference for precipitating out on bare metallic surfaces. Once precipitated, the asphaltenes build on themselves more rapidly than on clean surfaces. Depressurisation has also been found to cause precipitation of asphaltenes. Other causes of asphaltene precipitation include the presence of CO_2, acid (low pH), chemical shift that upset micelle (loss of light ends) and static storage. It is best to keep them in suspension or remove them in a pre-treatment step, as removal options are poor for precipitated asphaltenes (King, 2009).

Solvent separation and filtering are used as pre-treatment steps to remove asphaltenes from oil before they precipitate out in process equipment. Solvent separation is capable of removing a substancial amount of asphaltenes from feedstocks. Solvents such as n-heptane, ethyl acetate, n-pentane and n-hexane are used in ratio of residue and solvent of 1:50. The solution is filtered and the solvent is recovered through fractionation (Sharma, Bhagat & Erhan, 2007).

The determination of the precipitation onset point of asphaltenes is important to the study of asphaltene agglomeration. Precipitation is the formation of a semi-solid phase by the aggregation of solid particles. During precipitation particles with a diameter of approximately 1 micrometer are formed in a clustering process known as flocculation. When asphaltene particles form on a surface, deposition occurs. Deposition does not necessarily result from precipitation. There are three different phases during asphaltene precipitation from the bulk phase of the oil (Shadman et al. 2017).

- Asphaltene precipitation onset (APO)
- Asphaltene + Resin-flocculation onset (ARFO)
- Asphaltene + Resin-deposition onset (ARDO)

Asphaltene concentration does not have a significant impact on the precipitation onset point. The onset points of mixtures containing 0.1 g/l and 0.3 g/l of asphaltene (g)/toluene (l) without inhibitors are 52,5% and 52.4% respectively (Paridar et al., 2018). This difference is very small. The addition of an inhibitor 4-Dodecylbenzenesulfonic acid (DBSA) (500 ppm) which is a strong acid increases the onset point to 60.6%, which is a marked increase from

52.4%. That is 60.6% n-heptane (asphaltenes are insoluble in n-heptane) had to be added to the solution of 0.3g/l +500ppm DBSA before the precipitation onset point was reached (Paridar et al,. 2018). Therefore inhibitors/ dispersants are said to be effective in maintaining asphaltenes in suspension. Ahmed and Nassar (2011) confirm that inhibitors are present in lube oil.

Guichard et al. (2018) conducted an experiment on the diffusion/adsorption of asphaltenes through catalyst alumina supports. It was noted that an increase in temperature resulted in an increase in the amount of asphaltenes that adsorbed onto the alumina. This goes against normal absorption theory where it is expected that the absorption saturation should decrease with an increase in temperature. The contradictory result can be easily explained as asphaltenes have much lower average molecular weights at higher temperatures, which can speed up the diffusion process in comparison with the desorption behaviour. This phenomena will cause accelerated fouling in catalysts.

Asphaltenes are the heaviest and most polarisable molecules in oil, and their precipitation in reservoirs and pipe lines significantly inhibit production. Energy calculations reveal that Van der Waals forces are the primary and dominant force of attraction between asphaltene nano aggregates (Javanbakht et al. 2018).

Identifying the conditions under which asphaltenes precipitate from oils has challenged researchers over the past 12 years. The research has seeked to understand the effects that pressure, temperature and oil composition has had on asphaltene behaviour. It has been identified that the electro-kinetic behaviour of asphaltenes plays the biggest role in their stability and hence their tendencies to precipitate. It has been shown that asphaltene particles can be polarised and gain electric charge when exposed to an electrostatic field (Hosseini et al. 2016). It is important to note that this process is poorly understood. Hosseini et al. (2016) found that asphaltene molecules with higher complexity display faster aggregation behaviour when exposed to an electric field. Additionally they found that the aggregation rate was directly proportional to the number of hetero-atoms on asphaltene molecules. Hence it was concluded that an electrostatic field could highly affect the aggregation rate of asphaltene molecules. Figure 2.1 illustrates the complex nature of asphaltene molecules.

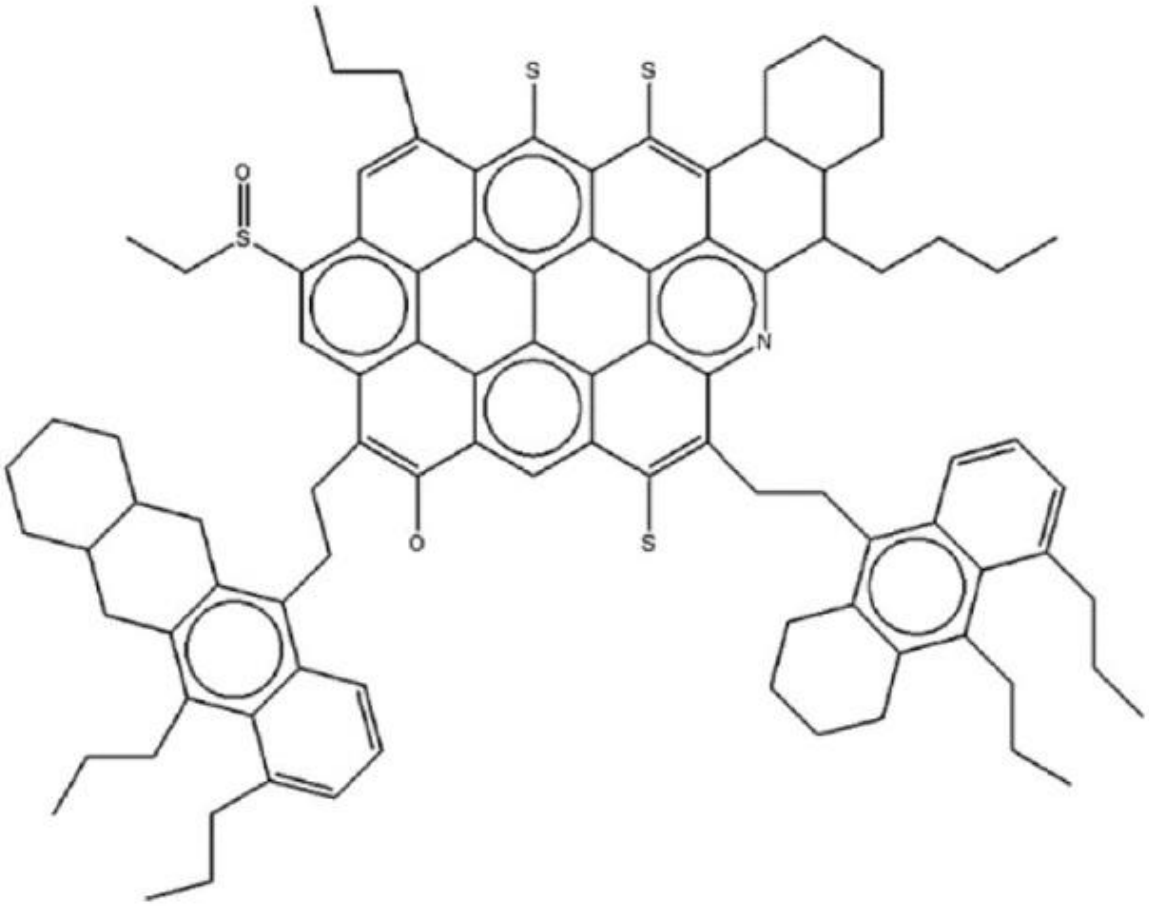

Figure 2.1 Example of the complex nature of asphaltene molecules (Hosseini et al., 2016)

Note that there are no specific names for the asphaltene molecules presented in figure 2.1.

There are a number of methods for determining asphaltene precipitation

- Viscosity measurement
- Filtration
- Heat transfer-based approach
- Electrical conductivity

2.4 Additive package

According to Nora Corporation (2003) lube oil additives start breaking down at temperatures above 200^{o}C, therefore it is desired that temperatures exceeding 200^{o}C be used in the new process. However 200^{o}C is too low of a temperature to result in the substantial viscosity reduction required. Studies involving viscosity reduction of used lubrication are very limited. Historically UALO has been refined for the use in blends and for feed to hydro-treating

plants in the production of base oil. Therefore existing processes employed by refineries to lower viscosities of petroleum were reviewed.

2.5 Refining petroleum

Distillation of crude oil does not produce products that are desired by the market place, therefore the molecular structure of petroleum "hydrocarbons" needs to be altered (Speight, 2008). Speight (2005) lists the following refinery processes used to alter and reduce the viscosities of petroleum: thermal cracking and catalytic cracking.

Petroleum is a complex mixture of mainly saturated hydrocarbon molecules and is the source of millions of tons of products used in everyday life. These products include textiles, plastics, adhesives, pharmaceuticals, rubbers and coatings to name a few. These products are produced by refining petroleum into the raw materials used in the manufacturing of such products. The refining step consists of breaking petroleum into smaller molecules and introducing new organic functional groups to allow the numerous desired chemical reactions to be carried out. One achieves this by using two types of cracking, thermal and catalytic. Thermal cracking mechanism depends on free radicals and the catalytic cracking mechanism depends on carbocations. They are both trivalent reactive species with one electron missing in the former and two in the latter (Green & Wittcoff, 2008). These species are depicted in figures 2.2 and 2.3.

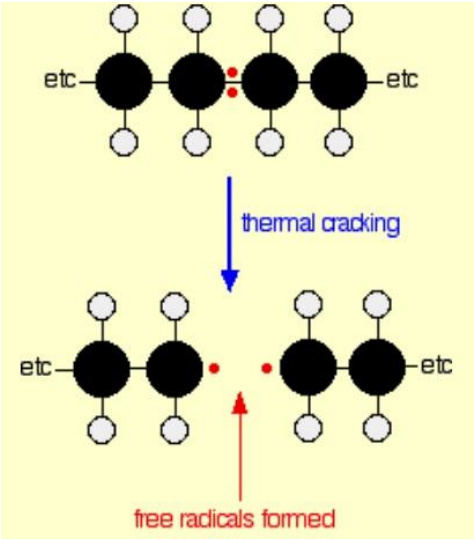

Figure 2.2 Thermal cracking (free radical intermediate) (Clark, 2003)

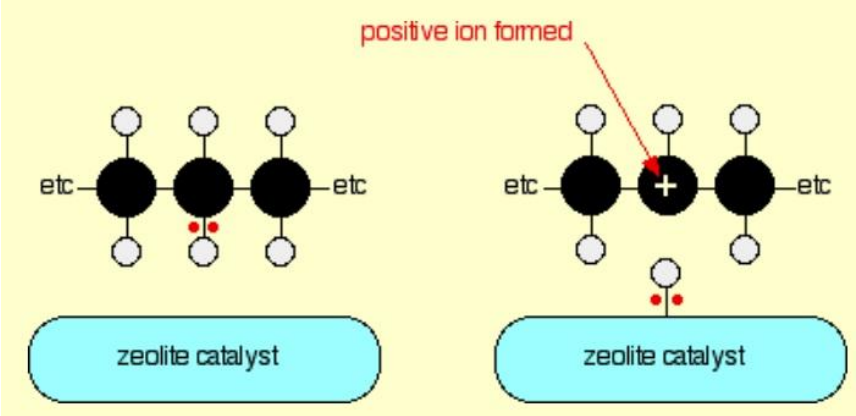

Figure 2.3 Catalytic cracking (carbocation intermediate) (Clark, 2003)

Thermal cracking is the oldest process (Green & Wittcoff, 2006) used to break down hydrocarbons into smaller molecules at temperatures in excess of 350^{o}C (Sadighi & Mohaddecy, 2013; Wilczura-Wachnik, 2009). Lower molecular mass molecules have lower viscosities than higher molecular mass molecules of the same nature (Kwaambwa et al., 2006). The thermal cracking process is endothermic and produces more moles of products than reactants, therefore, according to the Le Chatelier principle, heat must be supplied and the partial pressure of hydrocarbon (products) be kept low for cracking in the gas phase.

The radical mechanism consists of three phases; initiation, propagation and termination. Initiation consists primarily of the homolytic scission of a C-C bond producing two alkyl radicals.

$$CH_3CH_3 \rightarrow 2CH_3 \bullet -- (1)$$

The C-H bond is more stable and therefore has a higher bond dissociation energy (B.D.E) 340-380 kJ/mol compared to that of the C-C B.D.E of 290-380 kJ/mol. For this reason these kinds of bonds are less likely to break. The radical cleavage of C-C bonds leads to the formation of olefins (Angeira, 2008; Green & Wittcoff, 2006). Due to the large energies required, only a small amount of radicals are produced. The low concentration of radicals initially produced cannot account for the rapid breakdown of petroleum. This however can be accounted for in the propagation step (Green & Wittcoff, 2006).

Propagation involves a number of different reactions; hydrogen abstraction, addition, radical decomposition and radical isomerisation. The number of possible radicals and reactions

increases as the hydrocarbon chain length increases (Angeira, 2008; Robinson, 2007). Most importantly the propagation step produces more radicals.

$$CH_3 \bullet + CH_3CH_3 \rightarrow CH_4 + CH_3CH_2 \bullet --(2)$$

This process is known as the free radical chain reaction process, allowing a single initiation event to produce as many as a thousand olefin molecules. This accounts for the rapid break down of petroleum (Green & Wittcoff, 2006).

Termination is the opposite of initiation and involves the termination of radicals. Radicals terminate most commonly by reacting with each other, and less commonly by reacting with the metallic surface of the reactor wall. The former results in larger molecules (Angeira, 2008).

$$CH_3 \bullet + CH_3CH_2 \bullet \rightarrow CH_3CH_2CH_3 --(3)$$

$$CH_3CH_2 \bullet + CH_3CH_2 \bullet \rightarrow CH_2 = CH_2 + CH_3CH_3 --(4)$$

Molecular reactions such as dehydrogenation, isomerisation and cyclo-addition are less common in thermal cracking and more common in catalytic cracking (Angeira, 2008).

Main thermal cracking reactions

- Cracking of side chain free aromatic groups
- Dehydrogenation of naphthenes to form aromatics
- Condensation of aliphatics to form aromatics
- Condensation of aromatics to form higher aromatics
- Dimerisation or oligomerisation

The main process variables for thermal cracking reactions are (Sieli, 1998; Speight, 2008)

- Temperature (typical values of 455 – 540^{o}C)
- Pressure (typical values of 7 – 70 bar(g))
- Residence time (> 1 minute)

Rueda-Velasquez et al. (2017) sought to model the conversion of heavy oils to lighter feeds stock when subjected to thermal cracking. The heavy oils (HO#6 and HO#12) hence underwent thermal cracking to provide data for kinetic modelling. These trials covered a range of different temperatures and resident times. The pressure was kept constant. The impact of the severity of the reactions on the final viscosity of the product was assessed through the model. The mass balance of the model did not include the gases and coke produced during the thermal cracking trials as they were found to be negligible (less than 5%). Only liquid products were included. In tables 2.1 and 2.2 it can be seen that the reaction severity increases with longer resident times and the % conversion of heavy oil to lighter fractions with lower viscosities increases. The conversion of heavy oils in these reactions was between 8-23% for HO#6 and 9-17% for HO#12. The repeatability of the reactions was found to be good.

Table 2.1 Thermal Experiment, Summary of Results (adapted from Rueda-Velasquez et al., 2017)

Heavy oil	Temperature (°C)	Reaction Time (min)	Liquid Yields (%)	Conversion >524°C fraction (%)
HO#6	150	60	-	0
	350		-	10.7
	400	15	-	4.1
		30	-	7.8
		40	98.6	15.6
		50	98.2	17.1
			98.0	19.2
		60	98.4	22.2
			98.5	22.0
			99.1	25.1
		90	96.4	38.5
	450	15	94.3	47.3
		30	-	63.4
HO#12	150	60	-	0.6
	350		-	6.4
	400	15	-	4.7
		30	98.2	8.8
		40	98.5	16.6
		50	98.5	16.4
		60	98.3	15.2
	450	15	95.9	32.3
		30	88.3	63.8

Table 2.2 Concentrations on total mass basis of boiling fractions from the reactions of HO# 6 and HO# 12 at 400°C (adapted from Rueda-Velasquez et al., 2017)

Reaction time (min)	Overall mass concentration wt%			
	Naptha <177°C	Distillates 177-343°C	Gas Oil 343-524°C	Vacuum Residue >524°C
		HO#6		
Feed	2.1	14.1	22.6	61.2
15	2.6	14.5	24.2	58.7
30	2.7	15.5	25.4	56.4
40	2.9	16.5	25.7	53.5
50	2.8	16.6	25.6	53.2
60	2.7	17.0	26.3	52.6
90	3.8	20.0	25.6	47.0
		HO#12		
Feed	0	12.5	26.2	61.3
30	0.6	12.0	26.0	59.7
40	0.9	13.2	26.2	58.2
50	0.9	14.2	27.7	55.7
60	1.4	15.4	30.2	51.3

In table 2.2 the percentage of cuts can be viewed for reactions at 400°C at different resident times, both for HO#6 and HO#12. The longer resident times give the best conversion of heavy oil to lighter fractions, 20% conversion to distillates at 90 min for HO#6 and 15.4% conversion to distillates at 60 min for HO#12. In conclusion Rueda-Velasquez et al. (2017) found that it was possible to develop an accurate model to predict the viscosity of liquid products from the thermal cracking of heavy oils and much the same can be expected for UALO.

Corma et al. (2018) conducted thermal cracking experimentation on crude oil in the temperature range of 560-640°C. At 640°C they found that it was possible to convert 80wt% of the crude oil to vacuum gas oil with a resident time of 2 seconds. The products are equally distributed between gas, diesel and gasoline.

Alternatively solvent extraction can be employed as the majority of the base oil part of UALO is not spent because of the stability of the heavy compounds present in base oil. There are a number of different methods for removing the impurities from the unspent base oil, namely; distillation, acidic refining, clay treatment and hydrogenation. All these processes

give different yields and product quality. According to Osman et al. (2017), solvent extraction followed by adsorption was the more effective process for recycling waste lubrication oil. An experiment was conducted to identify the effectiveness of solvent extraction and adsorption on the recycling of UALO. In table 2.3 the different solvents that were used can be viewed,

Table 2.3 Solubility and dielectric constant of the three solvent mixtures (adapted from Corma et al., 2018)

Solvent Sample	Solubility (j/m^3)	Dielectric Constant
Toluene + butanol and methanol (A)	23.2	6.994
Toluene + butanol and ethanol (B)	22.2	6.993
Toluene + butanol and propanol (C)	21.5	6.992

and in table 2.4 it can seen that solvent C had the best yield but solvent A gave the best raffinate colour.

Table 2.4 Effect of different solvent mixtures on the refining of UALO (adapted from Corma et al., 2018)

	A	B	C
Raffinate (wt%)	48	63.3	81.1
Sludge (wt%)	52	36.7	18.9
Color (wt%)	Yellow	Black	Black

Activated alumina was used as the adsorbent and table 2.5 gives the results with the solvent and adsorbent being used in conjunction. It can be seen that the combination of solvent A and activated alumina gives the best yield and colour.

Table 2.5 Effect of activated alumina on the raffinates (adapted from Corma et al., 2018)

	A	B	C
Raffinate (wt%)	48	42.8	44
Sludge (wt%)	52	57.2	56
Color (wt%)	Yellow	Yellow	Yellow

Varying the solvent C to oil ratio only, did not improve the colour of the raffinate as can be seen in table 2.6

Table 2.6 Effect of solvent: oil ratio on the refining of used oil using solvent mixture C (adapted from Corma et al., 2018)

	01:01	01:02	01:03
Raffinate	81.8	70.1	55.6
Sludge	18.9	29.9	44.4
Color	Black	Black	Black

The physical and chemical properties of the raffinates produced during the trials can be viewed in table 2.7. It can be seen that although solvent C does improve on the colour of the oil, it does not result in the best chemical and physical properties for the raffinate. Ash is used as an example where 0.0094% , 0.046% and 0% is achieved for solvents A, B and C respectively. Osman et al. (2017) therefore concludes that solvent extraction followed by adsorption results in an excellent quality raffinate at yields between 44-81%.

Table 2.7 Physiochemical properties of UALO by solvent extraction and alumina treatment (adapted from Corma A et al., 2018)

Experiment	Origin sample	A	B	C
Density @ 15.5°C (cSt)	0.9116	0.8810	0.8847	0.8826
Viscosity @ 40°C (cSt)	107.48	51.66	76.02	83.67
Viscosity @ 100°C (cSt)	12.93	8.48	12.10	9.98
V.I	115.1	139.55	155.76	98.4
Pour point (°C)	0	3	3	0
Ash content (wt%)	1.05	0.0094	0.046	0
Sulfur content (wt%)	0.82	0.74	0.67	0.66

Additionally Mohammed et al. (2013) conducted a trial in the purification of used automotive lubrication oil using extraction and adsorption. N-hexane, 1-butanol, petroleum, ether, 1-hexanol, carbon tetrachloride and acetone were used as the solvents in the extraction, and the sorbents used were almond shell, walnut shell, eggshell and activated clay. The samples of oil were mixed with solvent-oil ratios of 1:1-1:3 for 15 minutes under continuous stirring and

after mixing it the samples were left for 24 hours at 30^{o}C to allow for extraction and flocculation. The solvent-oil solution was then separated from the sludge through filtration and the solvent recovered from the raffinate via vacuum distillation. The extracted oil was mixed with 15wt% of different adsorbents for 10 minutes (intense agitation). The oil was separated from the adsorbent through a final filtration step. The results from the trial can be seen in figure 2.4 and tables 2.8 – 2.9.

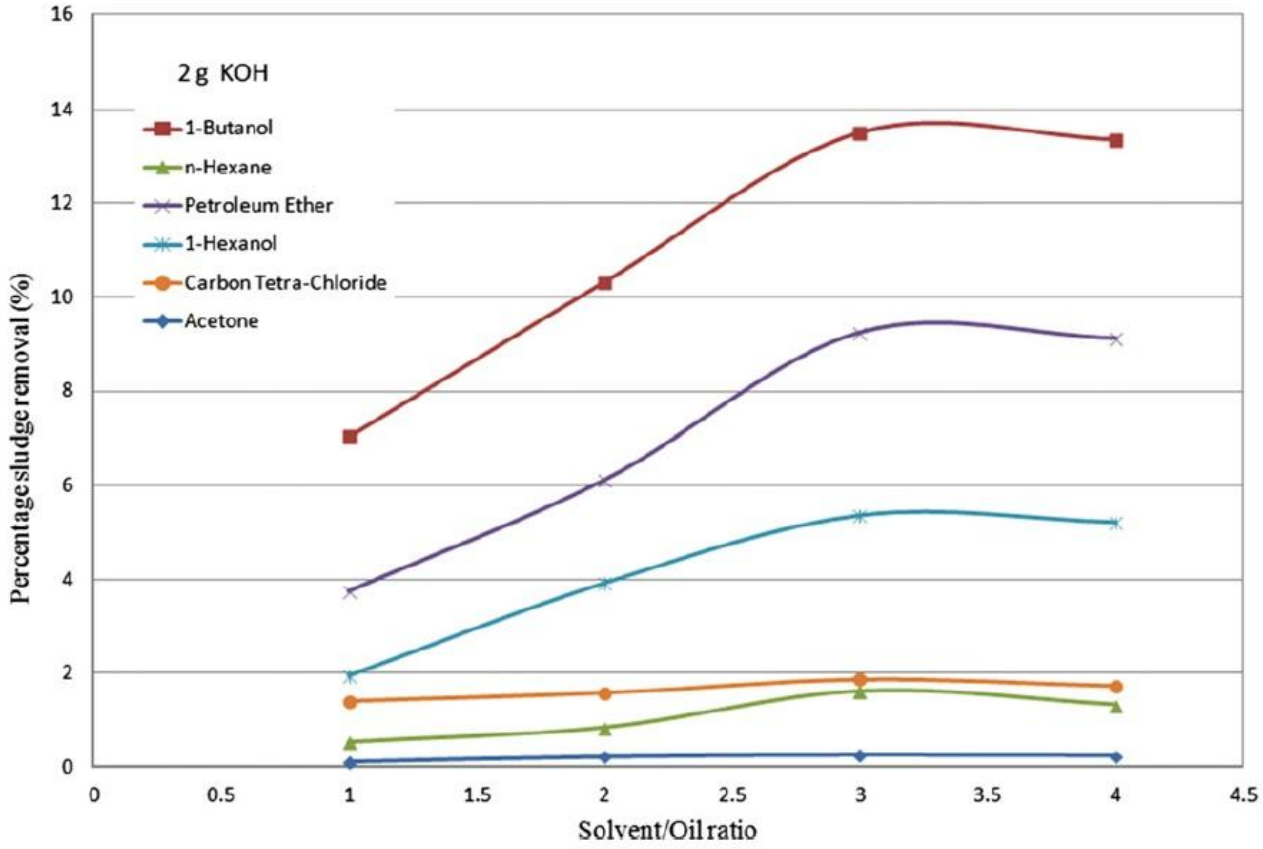

Figure 2.4 Percentage sludge removal vs Solvent/Oil ratio (Mohammed et al., 2013)

Figure 2.4 illustrates that the yield on the initial extraction step is above 90% but table 2.9 indicates that the final adsorption step reduces the yields to below 90%. The ash content was also unacceptably high for LO10.

Table 2.8 Properties of fresh, used and extracted oil with different solvent oil ratios (adapted from Mohammed et al., 2013)

Property	Fresh	Used	01:01	02:01	03:01	04:01
Density (kg/m^3)	895	912	909	905	899	903
Viscosity @ 40^{o}C (cSt)	131	38.3	49	61	72	69
Viscosity @ 100^{o}C (cSt)	14	6.1	7.1	8.7	10.3	9.6
Ash content (wt%)	0.463	0.952	0.843	0.706	0.515	0.564
Flash point (^{o}C)	243	178	195	211	220	218
Pour point (^{o}C)	-14	-6	-7	-8	-11	-10
Colour code	0.042	0.53	0.47	0.44	0.38	0.39

Table 2.9 Properties of fresh, used and extracted oil with different adsorbents (adapted from Mohammed et al., 2013)

Property	Fresh	Used	Clay	Egg	Almond	Walnut
Density (kg/m^3)	895	912	896	900	898	892
Viscosity @ 40^{o}C (cSt)	131	38	85	80	75	76
Viscosity @ 100^{o}C (cSt)	14	6	11	10	11	10
Ash content (wt%)	0.463	0.952	0.483	0.495	0.505	0.477
Flash point (^{o}C)	243	178	238	225	228	231
Pour point (^{o}C)	-14	-6	-13	-12	-12	-11
Colour code	0.042	0.53	0.12	0.25	0.15	0.21
Yield (%)			84	80	74	78

UALO can also be valorised through catalytic pyrolysis, where the UALO is heated in the absence of oxygen and thermally cracked into shorter lighter hydrocarbons that can be used as fuel. Iron based catalysts are being used in the upgrading of heavy petroleum residues with success. Ahmad et al. (2016) conducted a study in which two metal ions, barium (Ba^{2+}) and strontium (Sr^{2+}) were simultaneously doped into a magnetite matrix (Barium-strontium ferrite) and their catalytic effect on the conversion of UALO to diesel was explored. The elemental composition of barium-strontium ferrite can be viewed in table 2.10.

Table 2.10 The elemental composition of barium-strontium ferrite (adapted from Ahmed et al., 2016)

Element	Weight %
Carbon	5
Oxygen	24
Iron	60
Strontium	1
Barium	10
Total	100

UALO was fed into a reactor over 1-5wt% barium-strontium ferrite (BSFO). The mixture spent 90 min in the reactor at 500^{o}C before exiting and going through a condenser. The condensed liquid was collected as the product. A maximum overall conversion of 86.05% was obtained over the catalyst. This yield does not match the 90% required and this is because the properties of UALO ; low hydrogen/carbon ratio, high carbon residue, high density, large amount of heteroatoms, varnish, and large metal content have limited its conversion to a distillate via catalytic pyrolysis using a conventional catalyst (Khan et al. 2016). Khan et al (2016) conducted a study that looked at using magnetite ore as a new catalyst because it is one of the most abundant minerals, is nontoxic and requires no special methods of preparation. The work consisted of pre-treating the UALO with pre-baked clay (PBC) to remove soot, carbon, additives and metals. The optimum temperature and residence time was previously found to be 500^{o}C and 90min respectively (Khan et al., 2016). The runs consisted of varying the catalyst concentrations between 1 and 5%. The results can be seen in table 2.11.

Table 2.11 Yield of different pyrolysates as a function of natural magnetite concentrations (Khan et al., 2016)

Run	Catalyst Concentration (wt%)	Yield (%)			
		Overall	Liquid	Gases	Solid Coke
Thermal Catalyzed	No catalyst	99.20	95.60	3.60	0.80
	1	99.01	64.15	34.86	0.98
	2	98.04	62.09	35.94	1.96
	3	97.09	72.31	24.77	2.91
	4	96.14	70.30	25.83	3.86
	5	95.46	58.01	37.44	4.54

Reaction conditions used: Temperature: 500^{o}C, Residence time: 90 min.

It can be seen that the use of only 1% magnetite drops the liquid well below 90% to 64.15% and therefore the process is unsuitable. It must be noted that the absence of a catalyst resulted in a liquid yield of 95.6%.

The thermal treatment from literature appears to give the best results in terms of the valorisation of UALO. This statement is further substantiated by Bhaskar et al. (2004) who found that the increase of thermal treatment temperature decreases the sulphur content of UALO. At 200^{o}C the sulphur content decreased from 1640 ppm to 800 ppm, and at 400^{o}C the sulphur content decreased to 230 ppm. Figure 2.5 describes the sulphur reduction in UALO as the result of thermal treatment at different temperatures. It clearly shows that temperatures in excess of 300^{o}C have a great effect on the sulphur content of UALO. Figure 2.5 also shows that there is not a great deal of benefit in using residence times in excess of 1 hour, as at 400^{o}C the sulphur content at residence times of 1 and 10 hours was 270 ppm and 230 ppm respectively.

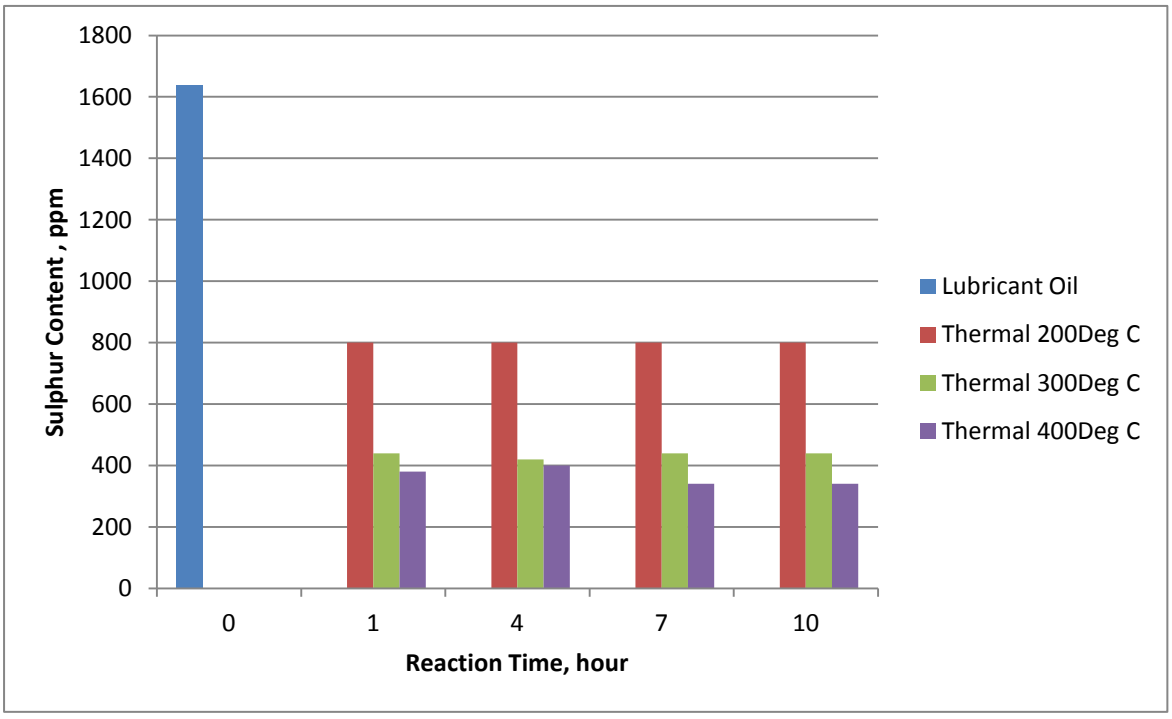

Figure 2.5 Sulphur content vs Reaction time (adapted from Bhaskar et al., 2004)

2.6 Emerging Technologies

Emerging technologies are starting to gather momentum as light crude oil reservoirs are becoming rare and because the current technologies are not completely adequate in processing heavy and extra heavy crude oils. These emerging technologies are summarised in table 2.12. They are designed to increase API gravity and decrease viscosity, sulphur, nitrogen and metallic compounds.

Table 2.12 Emerging technologies for heavy, extra-heavy crude oil processing (adapted from Castaneda et al., 2013)

No	Emerging Technology	Remarks
2.6.1	HCAT Process (Headwaters Heavy Oil)	Reported as a breakthrough process to convert low quality feedstock. Conversions up to 95% with a high reactor throughput. Uses a molecule sized catalyst and offers several significant advantages over supported catalyst based processes.
2.6.2	HTL (Heavy to Light) Process	Short contact time thermal conversion process that operates at moderate temperature and atmospheric pressure. Unique thermal cracking technology that solves some of the disadvantages of delayed coking, fluid coking and visbreaking processes.
2.6.3	GHU (Genoil Hydroconversion Unit) Process	Multiple fixed-bed reactor system. Feed stocks ranging from 6.5 to 17.5^{o}API. Only tested with feeds that have relatively low metals content.
2.6.4	Viscositor Process	Process for upgrading of heavy oil at the oil field: based on the atomization of oil with steam and further collision with heated sand in a high-velocity chamber to "crack" the oil where any catalyst is not required. Low severity makes this process technically feasible.

2.6.1 The Catalytic heavy oil upgrading process (HCAT)

The HCAT process chemically generates molecular sized catalyst inside the reactor through a conditioning process. The HCAT process along with the catalyst significantly improves the conversion of heavy fuel oil. The process holds several advantages over traditional supported catalyst systems; it offers non-deactivating catalyst, constant product quality, feedstock

flexibility and flexible conversion. The catalyst used in the process are oil-soluble such as iron pentacarbonyl and molybdenum 2-ethyl hexanoate. They offer coversions ranging between 60-80%. The process falls under Patent No. US 7,578,928 B2 (August 2009). Porvoo Refinery at South Jordan, Utah, was the first refinery to commercially implement the HCAT process.

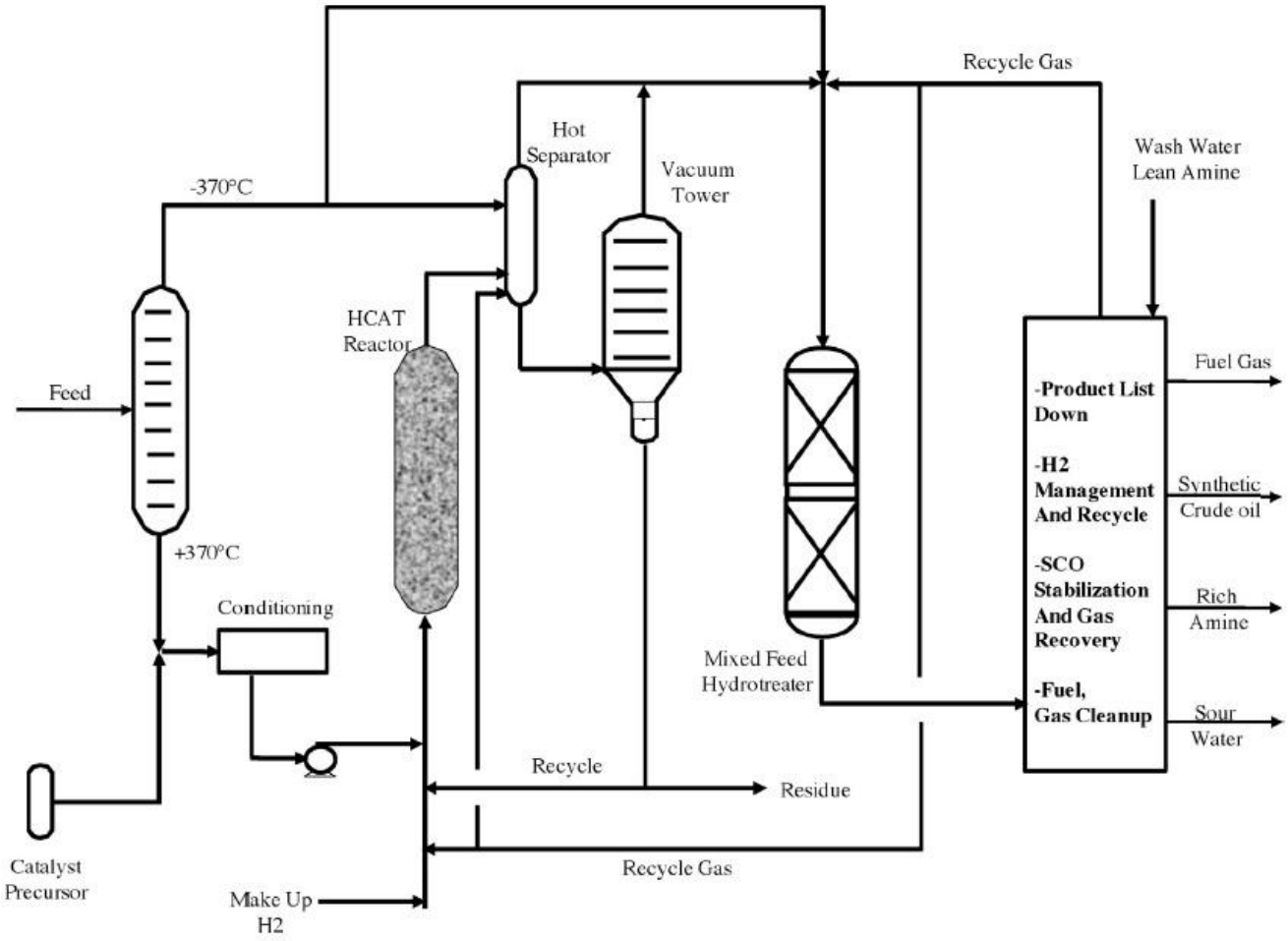

Figure 2.6 Schematic of the HCAT process (Castaneda et al., 2013)

2.6.2 The Heavy to Light (HTL) upgrading process

The HTL process uses a circulating bed of hot sand to heat the vacuum tower bottoms (VTB) feed stock and convert it to lighter products. In figure 2.7, the sand vaporises and cracks the liquid feed in the HTL reactor. The products exit the top as gas and are separated from the sand via a cyclone separator. The product stream is then quenched and condensed before it is

separated in a distillation column into its different fractions. The sand is sent to a furnace where the coke deposits are burnt off. The hot combustion gases reheat the sand and it is sent back into the HTL reactor. This process has some major draw backs; it requires large heat exchangers for heat recovery, has low volumetric yields of upgraded product and it produces large amounts of coke.

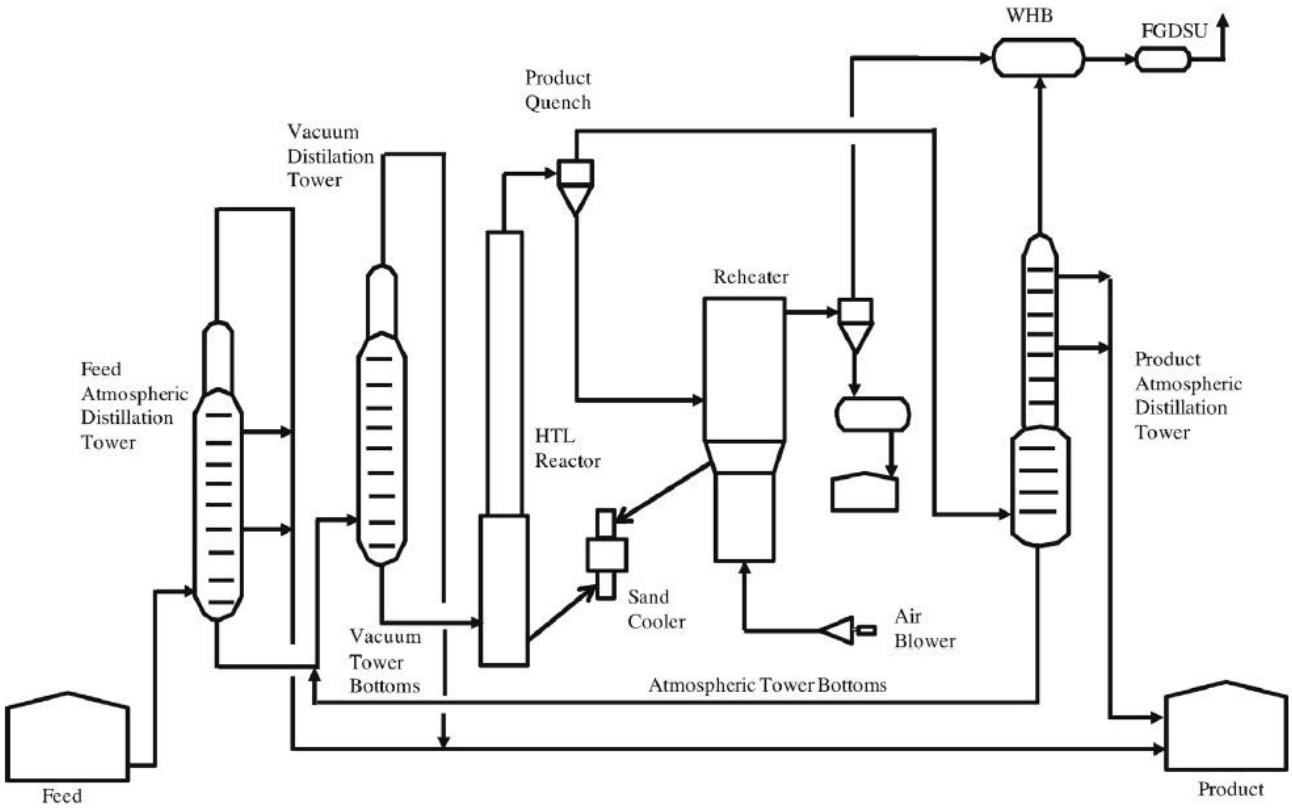

Figure 2.7 Schematic of HTL process (Castaneda et al., 2013)

2.6.3 Genoil hydroconversion process (GHU)

The Genoil hydroconversion process is a catalytic hydro-conversion process that upgrades heavy feedstock to a lighter product; it can achieve conversion rates as high as 70-90%. The GHU process consists of a hydro-metallisation (HDM) guard reactor followed by a second reactor using a combination of hydro-desulfurization (HDS) and hydro-denitrogenation (HDN) beds. Figure 2.8 shows a schematic of the GHU process.

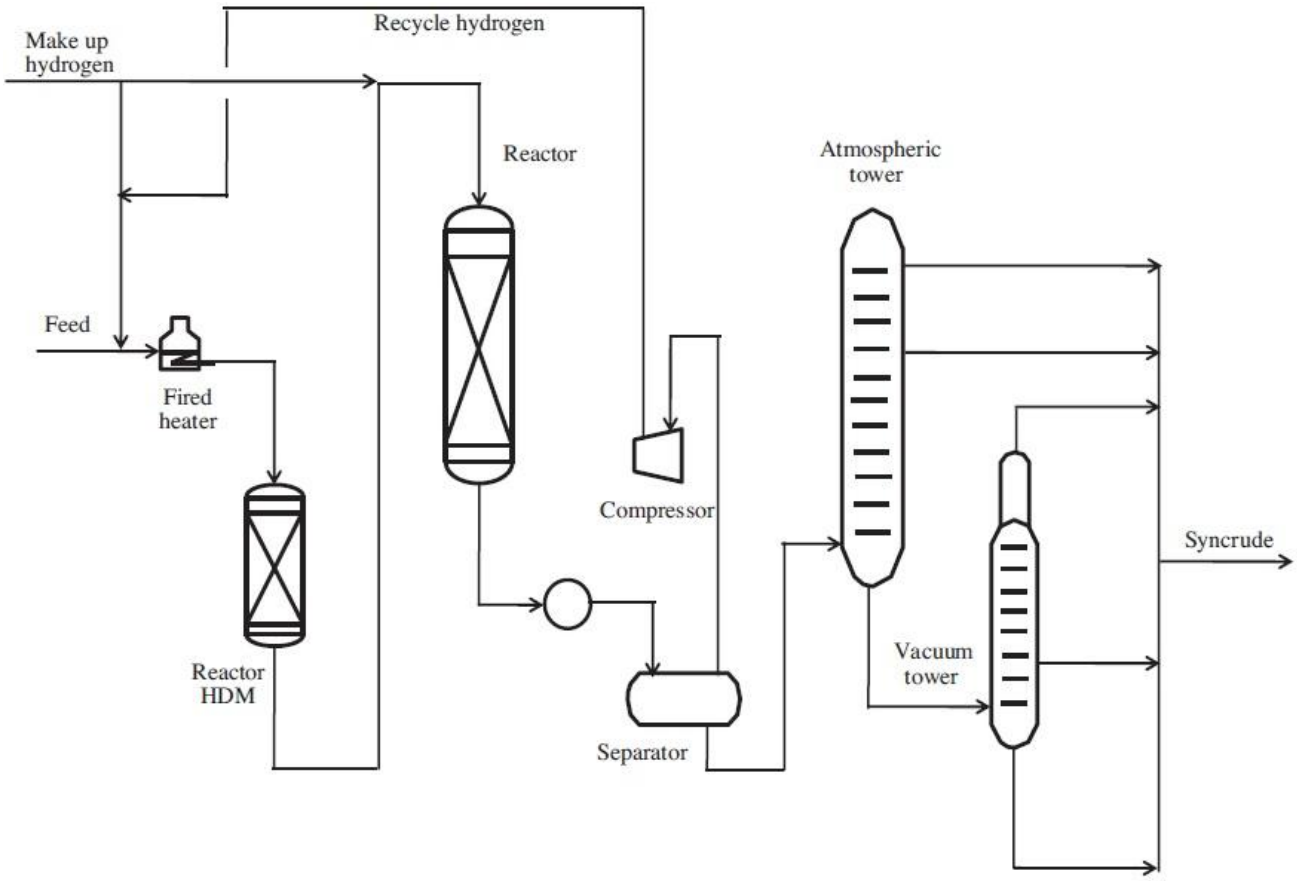

Figure 2.8 Schematic of GHU process (Castaneda et al., 2013)

The HDM bed removes 76-98% of the metals in the oil and the HDS and HDN beds remove 37-53% nitrogen, and 75-97% of the sulphur. Overall the process converts 37-88% of the residue (Castaneda et al., 2013).

2.6.4 Viscositor process

The viscositor process is a process for converting heavy oil at the oil field. The process involves the atomization of oil with steam and collisions with hot sand inside of a high-velocity chamber where the cracking of the oil occurs. The low temperature and pressure at which the cracking takes place makes it of particular interest. The basic schematic of the viscositor process is shown in Figure 2.9. Hot fine divided particles of sand heated by coke combustion in the reactor are pneumatically conveyed into the high-velocity collision chamber by hot combustion gases. Steam atomizes the heavy oil and the mixture is injected into the riser chamber where it collides with the particles and instant evaporation and cracking takes place (Castaneda et al., 2013).

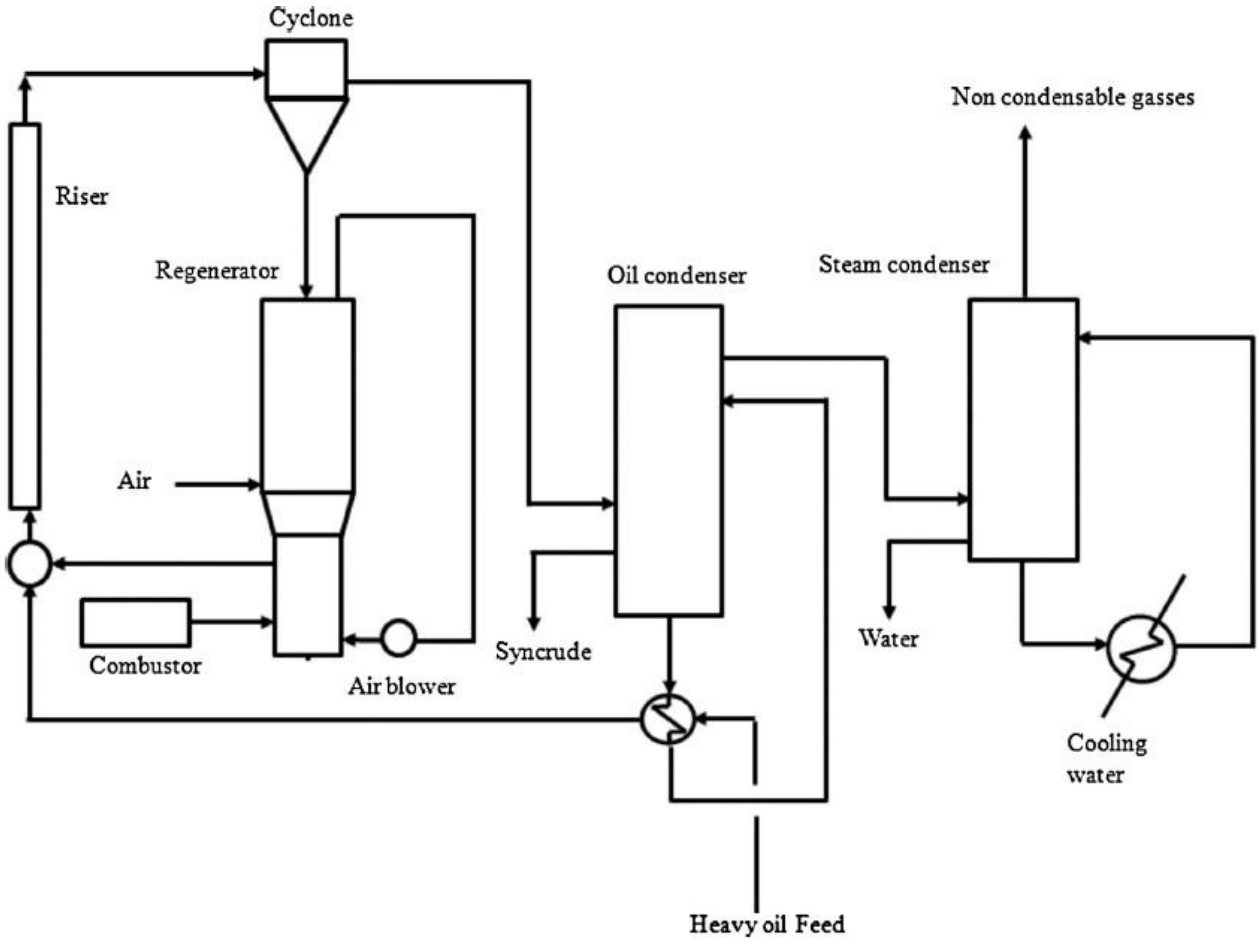

Figure 2.9 Schematic of the Viscositor Process (Castaneda et al., 2013)

The drawback of this process is that it is only capable of producing intermediate crude oils from heavy crudes. It is therefore meant to be used as a first processing unit in a refinery (Castaneda et al., 2013).

2.6.5 The process for intensive separation of raw hydrocarbon material process (PISRHM)

The PISRHM process is similar to that of a thermal cracking process and as stated previously, thermal cracking usually occurs at temperatures of 450^{o}C and above. When the critical energy is obtained and the oscillatory levels of the molecules are excited, the fracture of bonds occur (cracking). PISRHM is a thermo-mechanical process which initiates cracking under ultrasonic cavitation and oscillations which allows cracking to take place at a lower temperature of 380^{o}C (Zolotukhin 2004). The PISRHM process replaces thermal energy for

sound wave energy to reduce coking that occurs at higher temperatures. Using PISRHM, it is possible to obtain the following fractions from crude oil (Zolotukhin 2004).

Diesel fuel : 40-50%

Benzene : 20-30%

Heavy components : 20-30%

The HCAT, HTL and Viscositor emerging technologies all have the aim of upgrading extra heavy crude oil to a lighter crude oil that older refineries are accustomed to dealing with. They were designed to be placed upfront of a refinery as a pre-treatment step as to allow older refineries to continue to function and as normal, and as a result do not achieve the high conversion rates that are required in this work. The GHU process can be compared to that of a conventional hydro-treater and is therefore not suitable for the treatment of feeds with high impurity content such as UALO. The PISRHM process has not been proven on an industrial scale.

2.7 Existing petroleum refinery processes

Existing refinery processes are of particular interest as they are well know processes that have been proven and improved over decades. Literature so far has highlighted heat treatment as the best method for valorising UALO (Bhaskar et al., 2004; Khan et al., 2016; Nora Corporation, 2003; Rueda-Velasquez et al., 2017). Figure 2.10 gives the worldwide residue processing capacity distribution between the existing technologies.

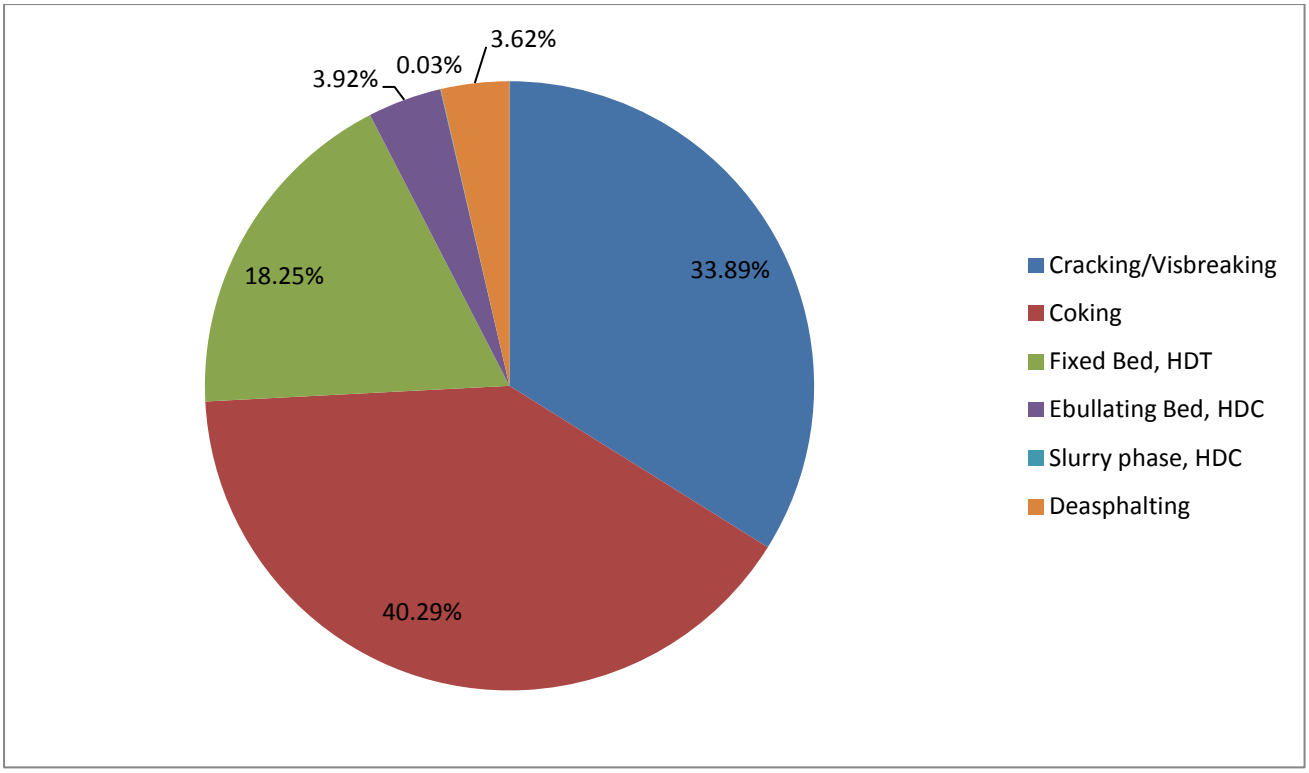

Figure 2.10 Worldwide distribution of commercial residue processing capacity (Castaneda et al., 2013)

The pie chart in figure 2.10 clearly shows that heat treatment is the most popular method for the upgrading of heavy residues, with 74% of the worldwide processing capacity.

2.7.1 Visbreaking

Visbreaking utilizes mild conditions to deliver mild thermal cracking, converting vacuum residue into lower viscosity fuel oil, regularly achieving conversion to gas, gasoline and distillates of 10-50%. This reduces the amount of cutter stock required to meet fuel oil viscosity specifications. There are two types of visbreaking units; the coil type and the heat soak type (Mohaddecy et al., 2011). The coil type operates at temperatures between 473-500^{o}C at short residence times of 1-3 minutes. 3-6 month run times are common before the coil needs to be de-coked. The main contributor to coke formation is the precipitation of asphaltenes (Agoretta et al., 2011). The heat soak type operates at temperatures between 427-443^{o}C at longer residence times utilizing an adiabatic drum after the coil. 6-18 month run times are common before the coil needs to be de-coked (Sepehr and Moheddecy, 2013). Most visbreakers inject steam into the coil to increase turbulence, improve the overall heat transfer

coefficient, lower the skin temperature and ultimately reduce coking. However excess steam will result in an annular flow regime which has been found to promote coking (Agorreta et al., 2011). The main variables in visbreaker operation are; temperature, pressure and residence time (Sieli, 1998).

Main reactions:

- Scission of a C-C bond
- Oligomerization and cyclisation to napthenes of olefinic compounds
- Condensation of cyclic molecules to polyaromatics

Side reactions:

- Formation of phenol, thiophenes, mercaptans and H_2S

Products depend on type of feedstock used. The following is a typical composition:

- 90-92% Fuel oil (lower viscosity)
- 5-7% Gas oil
- 2-3% Naphtha
- 1-2% Gas

2.7.2 Delayed Coking

Delayed Coking is a severe form of thermal cracking and is used to convert heavy low value residue into coke and valuable distillates. The distillate consists of fuel gas, naphtha and gas oil and contains no metals (Catala, 2009). It is an endothermic semi-continuous process with the furnace supplying most of the heat (Robinson, 2007). The furnace delivers the heated oil to an empty drum (coke drum) where coke deposition takes place. The distillate is drawn off the top and the coke cut out of the drum later by high pressure water (Catala, 2009). The most important operating variables in delayed coking are the drum temperature, pressure and recycle ratio. A furnace outlet temperature of 485-505^{o}C is maintained. A high drum pressure and recycle ratio are undesirable as it results in an increase in gas and coke yields (Stratiev et al., 2008). The ideal top drum pressure is 1-10 barg (Robinson, 2007).

2.7.3 Catalytic Cracking

Catalytic cracking, as the name suggests, utilizes a catalyst. In 1895 Ostwald proposed the following definition for a catalyst: 'a catalyst accelerates a chemical reaction without affecting the equilibrium'. Catalysts are selected for use in industry based on the following three important properties:

- Activity

The speed at which reaction/s proceed in the presence of a catalyst.

- Selectivity

Selectivity refers to the specific desired product produced by the use of a catalyst with a particular feed.

- Stability

Refers to the active life of the catalyst and is important to the economics of a process. Factors that affect stability include decompositions, coking, poisoning and reactant purity. The oil industry utilizes heterogeneous and homogenous catalysts. Of the two, the heterogeneous catalyst is the most widely used because it has a higher selectivity and repeatability (Wilczura-Wachnik, 2009). Additionally it is in the solid state and in a different phase to reactants and products, making separation easier (Wilczura-Wachnik, 2009).

The catalysis process is cyclic and consists of the following steps (Wilczura-Wachnik, 2009):

i. Reactants bind to one form of the catalyst
ii. Intermediate reactant complexes are formed, for example carbocations.
iii. The reaction proceeds
iv. Products are released from another form of the catalyst, thereby regenerating its intial state, returning the process to step i.

The end product of catalytic cracking varies and is dependent on the feed, nature of the catalyst and process conditions. There are predominantly two types of catalytic cracking. In the first type, larger molecules through the β-splitting reaction are broken down into smaller ones, for example the cracking of paraffins for the production of light olefins on a zeolite catalyst (Green & Wittcoff, 2006). Decreasing the pore diameter of zeolites increases the selectivity of light olefins; furthermore, H-ferrierite shows the highest olefin selectivity.

Catalytic cracking is preferred over thermal cracking in the production of olefins, in particular propylene as it produces higher yields (Komatsu, 2010).

The second type is designed to maximise branching through isomerisation, rather than cracking. The goal is to maintain the volatility of the molecular components while the intermediate carbocations produced favour the rearrangement of cyclo-aliphatic or linear molecules to highly branched saturated molecules (Green & Wittcoff, 2006). Carbocations, the intermediate to both types are produced over a positively charged zeolite catalyst.

A zeolite is a complex structure based on tetrahedral arrangements of alumina and silica. Each metal atom is surrounded by four oxygen atoms, bridging the metal atoms together into a complex network. Silicon is neutral in its tetravalent state; however alumina has a negative charge and requires a positive counterion like sodium to give the following general formula $Na_x[(AlO_2)_x(SiO_2)_y][H_2O]_y$ (Green & Wittcoff, 2006). These structures create microporosity in which channels similar in size to that of small hydrocarbons are formed. The channels are highly polar and a source of Bronsted acidity which is a potent cracking environment. The size of the channels dictates the maximum size of the molecules that can be catalyzed. The carbocations produced have two missing electons. Catalytic cracking reactions take place in the region of 500-800^{o}C (Green & Wittcoff, 2006), with side reactions viz. polymerization, cyclization and aromatization. These side reactions are the causes of catalyst deactivation (Wilczura-Wachnik, 2009).

Generally, catalytic cracking processes consist of three steps:

i. Reaction : Feed cracks via the catalytic cracking mechanism.
ii. Regeneration : The catalyst is reactivated by burning off coke.
iii. Fractionation : Products are separated into their separate fractions.

2.7.4 Fluidised catalytic cracker (FCC)

The fluidized catalytic cracker (FCC) is an example of such a process. It is one of the most popular and important processes used in refineries. Pre-heated feed is contacted with 650-800^{o}C highly active fluidized heterogeneous zeolite catalyst. Steam is also injected into the reactor to improve aeration (Nagiev et al. 2016). When the feedstock comes into contact with the hot regenerated catalyst, cracking occurs in ascending flow. As the catalyst becomes spent it is drawn off and sent for regeneration before being returned to the fluidised bed

reactor. Regeneration occurs by passing hot air over the catalyst removing adsorbed hydrocarbons and burning off coke (refer to figure 2.11). The combustion of the coke formed during the process provides the energy for the endothermic reactions that occur and for the vaporization of the feed stock. This also occurs in an ascending flow. The gases generated during the regeneration process are removed from the top of the regeneration chamber. The cracking takes place in a few seconds due to the highly active catalyst. The mixture of products and catalyst are separated in cyclones. The product is sent to a fractionation column and the catalyst to a fluidized bed regenerator. The FCC cracks larger molecules and converts them into light olefins (C_3-C_4) (Wilczura-Wachnik, 2009). FCC catalysts must possess the following physical and chemical properties; acid properties, high attrition resistance to impacts, stable at high temperatures, large pore sizes, resistant to poisoning, are of a form that allows for fluidization and produce a limited amount of coke (Alotaibi et al. 2018).

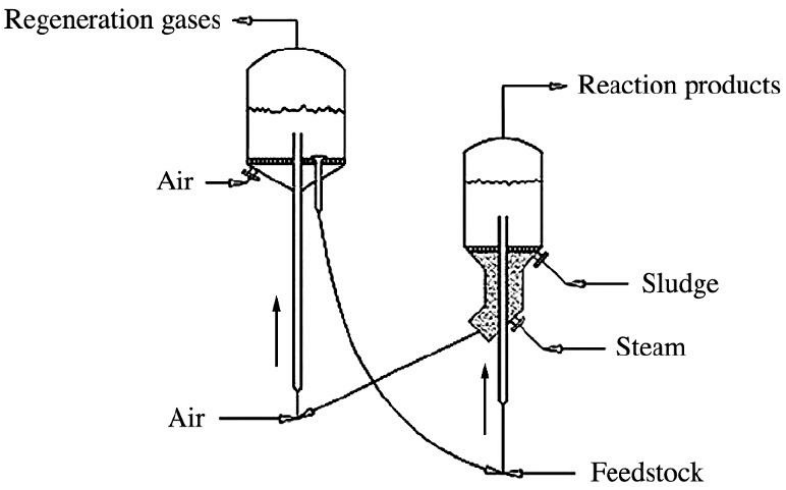

Figure 2.11 General view of reaction-generation catalytic cracking system (FCC) (Nagiev et al. 2016)

The FCC catalyst is composed of the following: zeolite (the active component), binder, filler catalyst, clay and the active matrix, as seen in figure 2.12.

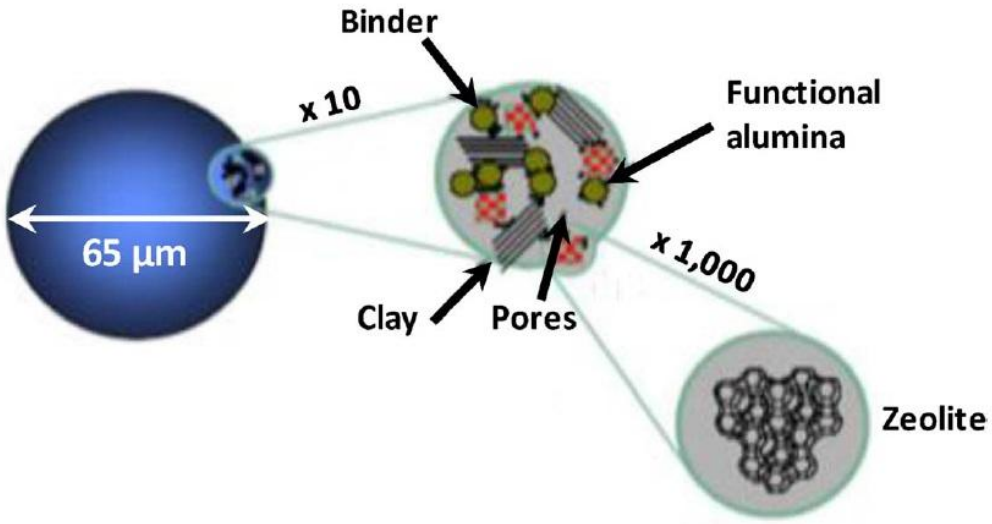

(A)

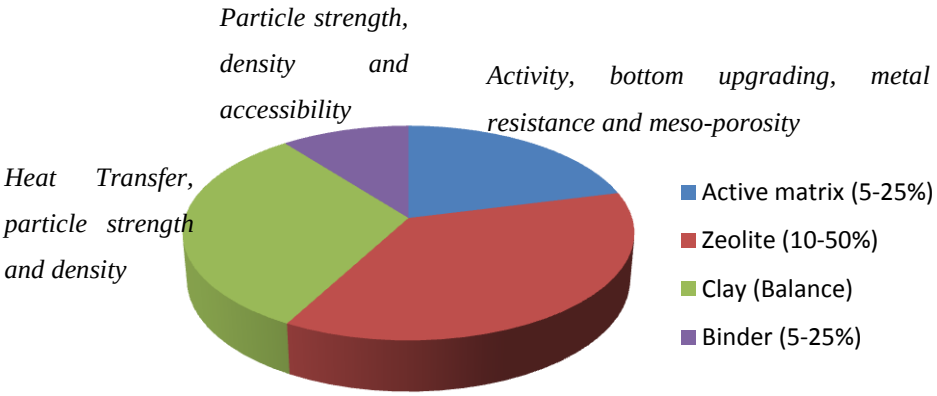

(B)

Figure 2.12 (A) Diagram of FCC catalyst (B) Composition and function of the catalyst (Adapted from Alotaibi et al., 2018)

Ultra-stabilized zeolite gamma (USγ) is used as the main active catalyst. It is made up of spherical particles which are suitable for fluidization in a circulating reactor. The zeolite crystals and clay particles are dispersed in the active matrix. This structure forms large voids and pores that are necessary for allowing mass transfer of large molecules from heavy feed stocks. The active matrix provides integrity, attrition resistance, porous structure and acts as a heat transfer medium.

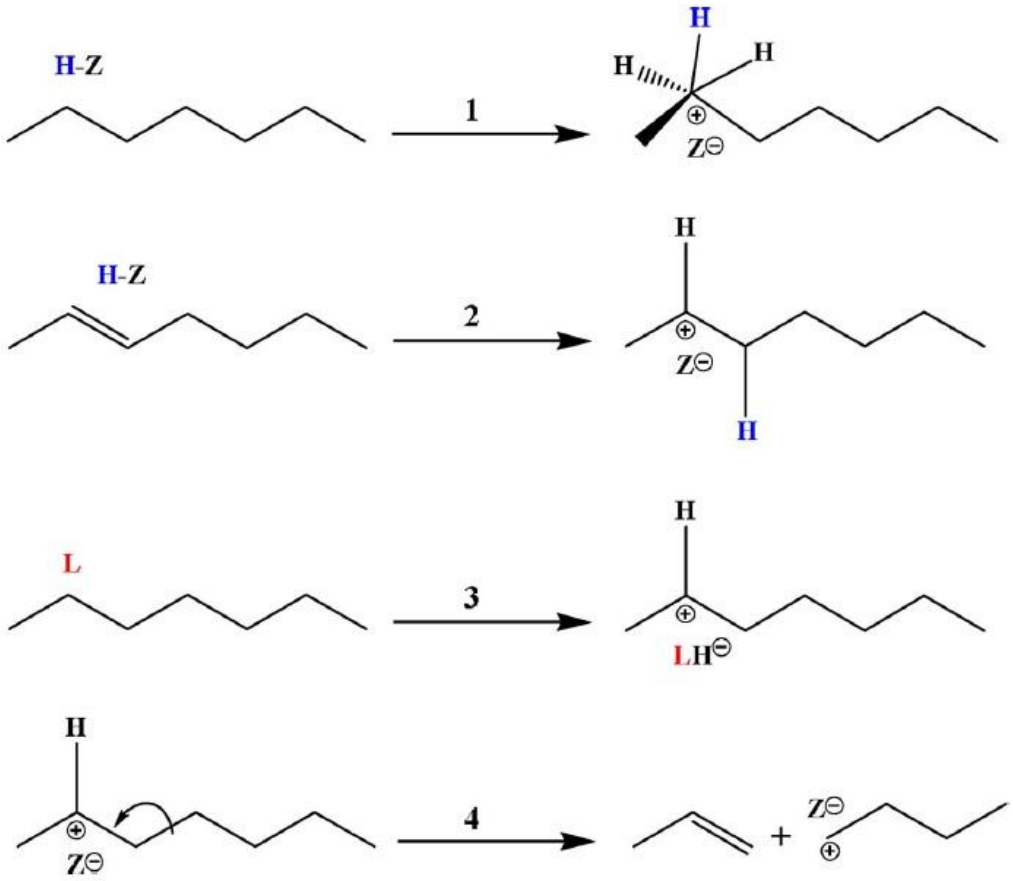

Figure 2.13 Catalytic cracking reaction pathways (Alotaibi et al., 2018)

Figure 2.13 shows the catalytic cracking reaction pathways over a zeolite catalyst. Reaction 1 displays the interaction between the catalyst and the hydrocarbon. Reaction 2 and 3 show the carbedium formation through proton and hydride formation and reaction 4 shows the β-scission to form a primary carbedium.

Recently there has been a lot of advancement in FCC catalyst design. The main goal has been to decrease hydrogen transfer reactions (coking) while keeping high olefin yields. These methods and parameters include (Alotaibi et al. 2018):

- ZSM-5 catalyst with optimised silicon/aluminium ratios
- Nano-size crystal ZSM-5 catalyst
- Hydrothermal deactivated ZSM
- Treating ZSM-5 with phosphorus
- The addition of a rare-earth, alkali metals and/or alkali earth metals

- The addition of some transition metals with an optimum balance between dehydrogenation activity of the metal and acid function of the HZSM-5 zeolite shape
- ZSM-5 with hierarchical pore structure which can be introduced by a number of different methods (steaming, acid leaching etc)

However these methods only enhance the conversion of conventional crude oil to light olefins. Unconventional oils such as heavy feed stocks, residues and bitumen remain a big challenge (Alotaibi et al. 2018). The properties of these unconventional oils such as high molecular weight, low hydrogen to carbon ratio, high contents of metals and unsaturated poly-aggregate asphaltenes calls for more intensive research into advancements in catalytic systems.

The addition of rare earth metals to Y zeolite catalysts increases the activity per unit weight of zeolite (Sousa-Aguiar et al., 2013) and as a result hydrogen transfer in catalytic cracking processes is enhanced. Thermal deactivation is a well known occurrence in catalysts that operate at high temperatures. This thermal deactivation occurs in FCC plants whose catalysts operate at temperatures between 500-800^{o}C. The introduction of rare earth metals to Y zeolite catalysts (around 10 wt%) (Sousa-Aguiar et al., 2013) has been found to be good agents for delaying this thermal deactivation.

The presence of Nickel and Vanadium are the biggest culprits when it comes to poisoning (permanently deactivating) catalytic cracking catalyst (Sousa-Aguiar et al., 2013)

The best way to prevent coking in an FCC unit is to avoid heat loss and dead spots. Heat loss can be avoided by insulating the process, and dead spots can be prevented by using steam to sweep out stagnant areas. Heavy oil in FCC units are the most likely to be condensed to form coke. It is therefore desired to convert the heavier oil to lighter hydrocarbons as completely as possible (Lan et al., 2009). Experiments have shown that heavy oil was harder to crack and produced more coke in the FCC process due to the following properties; higher density, carbon residue and lower H/C ratio. The temperature had the largest effect on the heavy oil conversion. The increasing temperature led to a much larger heavy oil conversion and coke yield. The optimum temperature for heavy oil conversion was found to be 500^{o}C (Lan et al., 2009).

2.7.5 Steam Catalytic Cracking (SCC)

In the SCC process, heavy oil is cracked in the presence of steam and a catalyst. It is a combination of thermal and catalytic cracking and may be the most reliable process in the upgrading of heavy fuel. Steam cracking of 2-methylpentane over USY catalyst revealed that steam enhances isomerisation and hydrogen transfer reactions (Alotaibi et al., 2018). Refer to figure 2.14 for a typical steam cracker consisting of a cracking furnace, quench and fractionators. The feed along with steam are fed into a 45-90 m long tubular reactor. Within a second the mixture is heated to between 700-900^{o}C at a pressure of 7-14bar (Alotaibi et al., 2018). After exiting the reactor the product stream is rapidly quenched to prevent further cracking and polymerization reactions. Due to the high temperatures required in steam cracking, it is one of the most energy intensive processes in a refinery.

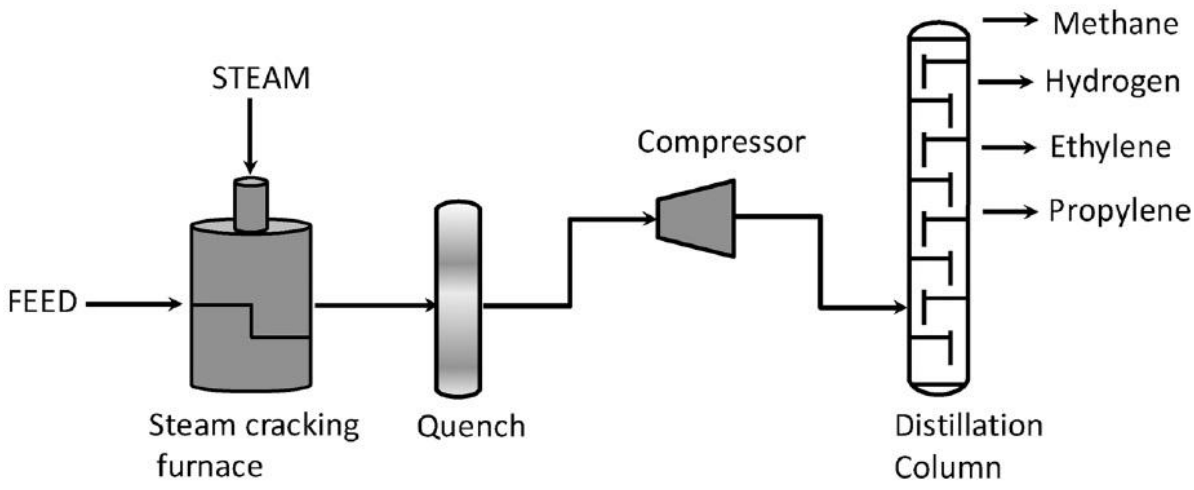

Figure 2.14 Diagram of a typical steam cracker (Alotaibi., 2018)

In cracking, the colloidal suspension of asphaltenes and resin compounds precipitate out and form highly linked amorphous coke structures (a porous hard, involatile residue consisting mostly of carbon) (Green and Wittcoff, 2006). These compounds are also subjected to cleavage of aliphatic groups (Stratiev et al., 2008).

2.7.6 Thermal oxidative cracking (TOC)

The thermal decomposition of hydrocarbon (thermal cracking) occurs at high temperatures (350-600^{o}C) and medium to high pressures. Thermal oxidative-cracking (TOC), as the name

suggests, takes place in the presence of atmospheric oxygen at atmospheric pressure. The reaction takes place in the vapour phase and the amount of energy required is supplied by the oxygen in the air oxidising the hydrocarbons. Oxidation is an exothermic reaction. The flow rate of air used was varied to maintain the reaction temperature. The TOC mechanism consists of three stages; origin of the chain, continuation of the chain and breaking of the chain (Goncharov & Belyaevskii 2005).

The origin of the chain stage consists of the formation of radicals from the monomolecular decomposition and bimolecular interactions of particles. Therefore the chain reaction begins, for example, when pentane undergoes monomolecular decomposition with respect to the C-C bond in the β-position toward the radical centre:

$$CH_3CH_2CH_2CH_2CH_3 \rightarrow CH_3CH_2 \bullet + CH_3CH_2CH_2 \bullet --(5)$$

The main difference between TOC and thermal cracking is the existence of oxygen in the system. The Bach-Engler theory describes the following; an oxygen molecule is attached to a substance that can oxidised without dissociating and forming an oxide molecule (Goncharov & Belyaevskii 2005).

$$CH_3CH_2CH_2 \bullet + \bullet OO \bullet \rightarrow CH_3CH_2CH_2OO \bullet --(6)$$

$$CH_3CH_2 \bullet + \bullet OO \bullet \rightarrow CH_3CH_2OO \bullet --(7)$$

Oxygen molecules become active during the TOC process by the breaking of one bond, forming bi-radicals.

$$O = O \rightarrow \bullet OO \bullet --(8)$$

This oxygen bi-radical is responsible for the bimolecular interactions between particles. The stage of chain continuation consists of the splitting and isomerisation of the free peroxide radicals.

$$CH_3CH_2OO \rightarrow \bullet CH_2CH_2OOH --(9)$$

$$\bullet CH_2CH_2OOH \rightarrow CH_3CHOOH \bullet --(10)$$

Monomolecular decomposition results in the formation of new radicals, aldehydes and ketones. In near complete thermal oxidation original free radicals enter into reaction with the products that are obtained (Goncharov & Belyaevskii 2005).

$$CH_3CHO + CH_3CH_2 \bullet \rightarrow CH_3CH_3 + CH_3CO \bullet --(11)$$

The final stage of chain breaking consists of disproportionation, where the reactive free radicals begin to react with each other causing chain breakage.

$$CH_3CH_2CH_2 \bullet + CH_3 \bullet \rightarrow CH_3CH_2CH_2CH_3 --(12)$$

$$CH_3CH_2 \bullet + CH_3 \bullet \rightarrow CH_3CH_2CH_3 --(13)$$

Longer chain hydrocarbon molecules result in the formation of a greater amount of different molecules. Molecules like alkanes, alkenes, alkynes, hydrogen and carbon monoxide. At lower pressures and temperatures alcohols, aldehydes, ketones, acids, phenols, etc are formed.

Advantages of the TOC process (Goncharov & Belyaevskii 2005)

- Takes place at atmospheric pressure
- No expensive catalyst
- High yields of gaseous products
- No coke formation

The high yields of gaseous products make the TOC process undesirable for the use in the valorisation of UALO as the production of gas reduces the yield of LO10.

2.8 Heating furnace

It is widely known that furnace coil failure is a common occurrence in thermal cracking processes and all refinery processes require the use of a furnace. Therefore, research into furnace technology is a continuous process due to the before mentioned and the high-energy consumption and the, capital and maintenance cost of the current cracking furnace. The heating of feed for cracking of heavy hydrocarbons in the production of lighter products is mainly carried out in fired heaters with tubular coils. A modern furnace design incorporates a rectangular firebox with vertical tubes in the centre between two radiating refractory walls and operates at temperatures in the range of 1200^{o}C. The majority of heat transfer takes place via radiation, while convection plays a minor role. The heat flux must be uniform in the

firebox or over-cracking will occur, shortening the coil life. Small errors in equipment design/sizing can translate to tens of millions of Rands in expenses (Robinson, 2007).

These processes usually have a service life of 100 000 hours but coils on average fail between 4000-6000 hours of operation. The presence of hydrogen sulphide in low chrome steel at temperatures between 425-455^{o}C may result in corrosion rates in coils as high as 0.6 mm/year. However, the presence of an abrasive process fluid that prevents the formation of passive corrosion films will result in a corrosion rate substantially higher than 0.6 mm/year. It is therefore recommended that in furnace coils where the partial pressure of hydrogen sulphide is greater than 0.1 kPa, higher chrome steels (8-9% chrome) be used instead of low-chrome steels (5% chrome) (Medvedeva 1998).

Annular flow type regimes must be avoided in the heating coil. Annular flow consists of gas flowing at high speeds through the centre of the pipe while oil separates and circulates over the coil walls, where velocities approach zero. Therefore overheating and coking tend to occur. It is a well known fact that this type of flow regime increases coking rates (Agorreta et al., 2011).

Coil design parameters

i. Low pressure
   - Promotes the formation of olefins

ii. Low hydrogen partial pressure
   - Prevents hydrogenation and promotes the formation of olefins

iii. Short residence time
   - Prevents condensation reactions (< 0.5 seconds)

2.9 Chapter Summary

All the studies discussed above have shown cracking to be the preferred process for producing low viscosity products from heavy feedstocks at high yields. The main two avenues of cracking include thermal cracking and catalytic cracking. Thermal cracking employs high temperatures to break large molecules into smaller ones, thereby reducing the viscosity. This takes place via the free radical mechanism. Catalytic cracking employs a catalyst to achieve the same, but at higher selectivity via the catalytic cracking mechanism.

Table 2.13 Yield comparison between different thermal processes (adapted from Goncharov & Belyaevskii, 2005)

Reaction Product	Thermal Processes			
	Pyrolysis	Catalytic cracking	Cracking under pressure	Thermal-oxidative cracking
	Yield of products (wt%)			
H_2	0.8	1.2	0.4	1.3
CH_4	10.1	18.7	4	18.5
C_2H_6	2.9	4.6	1.8	3.4
C_2H_4	28.5	34.1	0.3	18.4
C_2H_2	0	0.7	0	20.5
C_3H_8	0.4	0.5	1.5	3.6
C_3H_6	10.9	12.9	0.8	12.9
ΣC_4	3.5	5.6	0.5	3.5
Total wt% conversion to Gas	**57.1**	**78.3**	**9.3**	**82.1**

Table 2.13 indicates that cracking under pressure produces the least amount of gas 9.3% and therefore produces a product with a liquid yield of above 90%. The other thermal processes produce a large amount of gas, as much as 82.1% with thermal-oxidative cracking and 78.1% with catalytic cracking.

However, current literature does not discuss the cracking of UALO for the production of LO10. Due to the lack of literature, the following cracking process variables are unknown namely temperature, pressure and residence time. Current refinery processes and variables will be used as guidelines.

In the valorisation of UALO, the interest lies in viscosity/impurity reduction and the degree of cracking. There is no interest in the molecular make up of the final product. The amount of saturates and olefins are immaterial, therefore the selectivity supplied by a catalyst is not required. Additionally the low liquid yield found in catalytic cracking and the high content of impurities found in UALO renders the use of catalysts impractical as rapid fouling and low liquid yields would result. Therefore catalytic cracking is not a viable option, leaving thermal cracking as the only option. The presence of the impurities is the result of the additive package in lubrication oil and side reactions in internal combustion engines. The two main

contributors to the ash content are the additive package and asphaltenes produced via the side reactions.

The additive package starts to break down at temperatures above 200^{o}C. Asphaltene micelles are disturbed at high temperatures, causing the asphaltene particles to agglomerate and drop out of suspension. Therefore the use of thermal cracking in the treatment of UALO will result in a substantial ash and viscosity reduction in the said oil. The three most important properties of thermal cracking are temperature, pressure and residence time. However these are all unknown in the production of LO10 from UALO. This work will therefore seek to identify the optimum temperature, pressure and residence times at which LO10 can be produced from UALO at sufficiently high yields.

There are two main types of thermal cracking namely, visbreaking and delayed coking. Visbreaking has been decided upon, as the formation of coke in delayed cracking is undesirable as it reduces the yield of LO10. There are two well documented types of visbreaking processes; the coil type and the heat soak drum type. The heat soak drum type has been decided upon as it requires milder temperatures and has longer expected run times before decoking of the coil is required.

The coil design is an intricate part of the process in terms of heating and run length, but does not contribute significantly to the degree of cracking. The cracking in a heat soak drum type visbreaker takes place in the heat soak drum. Therefore in terms of the scope of this thesis, only the conditions in the heat soak drum was investigated. A heat soak drum bench top test rig was designed and set up in order to conduct experimentation and identify the optimum thermal cracking temperature, pressure and residence time. Literature (Agorreta et al., 2011; Mohaddecy et al., 2011; Siele, 1998) describes the following process conditions for the heat soak drum type visbreaker:

Temperature : > 350^{o}C

Pressure : 7 – 70 barg

Residence time : > 3 min

These conditions were used as guidelines when conducting the design of experiment.

3 Methodology

3.1 Introduction

As previously stated, one of the objectives of this thesis is to identify a process to produce LO10 from UALO at a yield greater than 90%. An inductive approach was adopted for this work because no open literature on the production of LO10 from UALO could be. A literature review was carried out on UALO. The conclusions from literature revealed the challenges associated with the conversion of UALO to LO10. These challenges led to the development of the research questions as well as the subset of questions listed below.

a. How to breakdown the additive package found in used automotive lubrication oil?
b. What existing oil refinery processes will reduce the viscosity of UALO and break down the additive package?
c. What are the critical operating variables?
d. How do these variables affect the viscosity yield and additive package?
e. What are the optimum values for the critical operating variables?

Based on the research questions, the research paradigm required was both qualitative and quantitative. Qualitative in that a literature review on existing technology was carried out in identifying a suitable process and the critical operating variables, and quantitative in that experimentation was carried out on the process in answering the remaining research questions (iv and v).

3.2 Process

Thermal cracking has been traditionally used in oil refineries to break down hydrocarbons into smaller molecules thereby reducing viscosity at temperatures in excess of 350^{o}C (Sadighi & Mohaddecy, 2013; Wilczura-Wachnik, 2009) and according to the Nora Corporation (Nora Corporation, 2003), lube oil additives start breaking down at temperatures above 200^{o}C. This is the reason thermal cracking was selected for the conversion of UALO to LO10; it will both reduce the viscosity and break down the additive package found in UALO. Furthermore the

Drum Heat Soak Type Visbreaker was selected as the process because it utilizes mild conditions to deliver mild thermal cracking (Mohaddecy et al., 2011) with a long coil life of 6-18 months (Sepehr and Moheddecy, 2013).

3.3 Process Variables

Analysis of literature revealed that thermal cracking is reliant on the following three critical variables (Sieli, 1998; Speight, 2008):

- Temperature (typical range: 455 – 540^{o}C)
- Pressure (typical range: 7 – 70 bar(g))
- Residence time (> 1 minute)

It was for this reason that temperature, pressure and residence time were selected as the critical process variables to be investigated.

3.3.1 Temperature range

The temperature range investigated was set at 200-500^{o}C with 200^{o}C being the temperature at which the UALO additive package starts breaking down (Nora Corporation, 2003), and 500^{o}C being the temperature at which the best results were achieved in the upgrading of UALO (Ahmed et al. 2016; Khan et al. 2016; Lan et al., 2009).

3.3.2 Pressure range

The pressure range investigated was set at 0-15 bar(g) with 0 bar(g) being limited by ambient atmospheric conditions, and 15 bar being above the maximum pressure of 10 bar. Pressures above 10 bar were found in literature (Robinson, 2007) to be the points at which the gas make dramatically increased and oil yields decreased, which in this work was not desirable.

3.3.3 Residence time range

The residence time range investigated was set at 20-60 min with 20 min being limited by minimum desired time and 60 min being limited by the heat soak vessel size at full scale production. Literature states that the optimum residence time range was between 1- 90 min

(Sieli, 1998; Speight, 2008; Kahn et al. 2016; Rueda-Velasquez R et al., 2017). The residence time range in this work therefore fell within the recommended residence time range stated in literature.

The range of the critical operating variables investigated was adopted from literature which is presented below:

Temperature (^{o}C) : 200-500

Pressure (bar) : 0-15

Residence time (min) : 20 – 60

3.4 Apparatus

A Heat Soak Drum benchtop test rig was built.

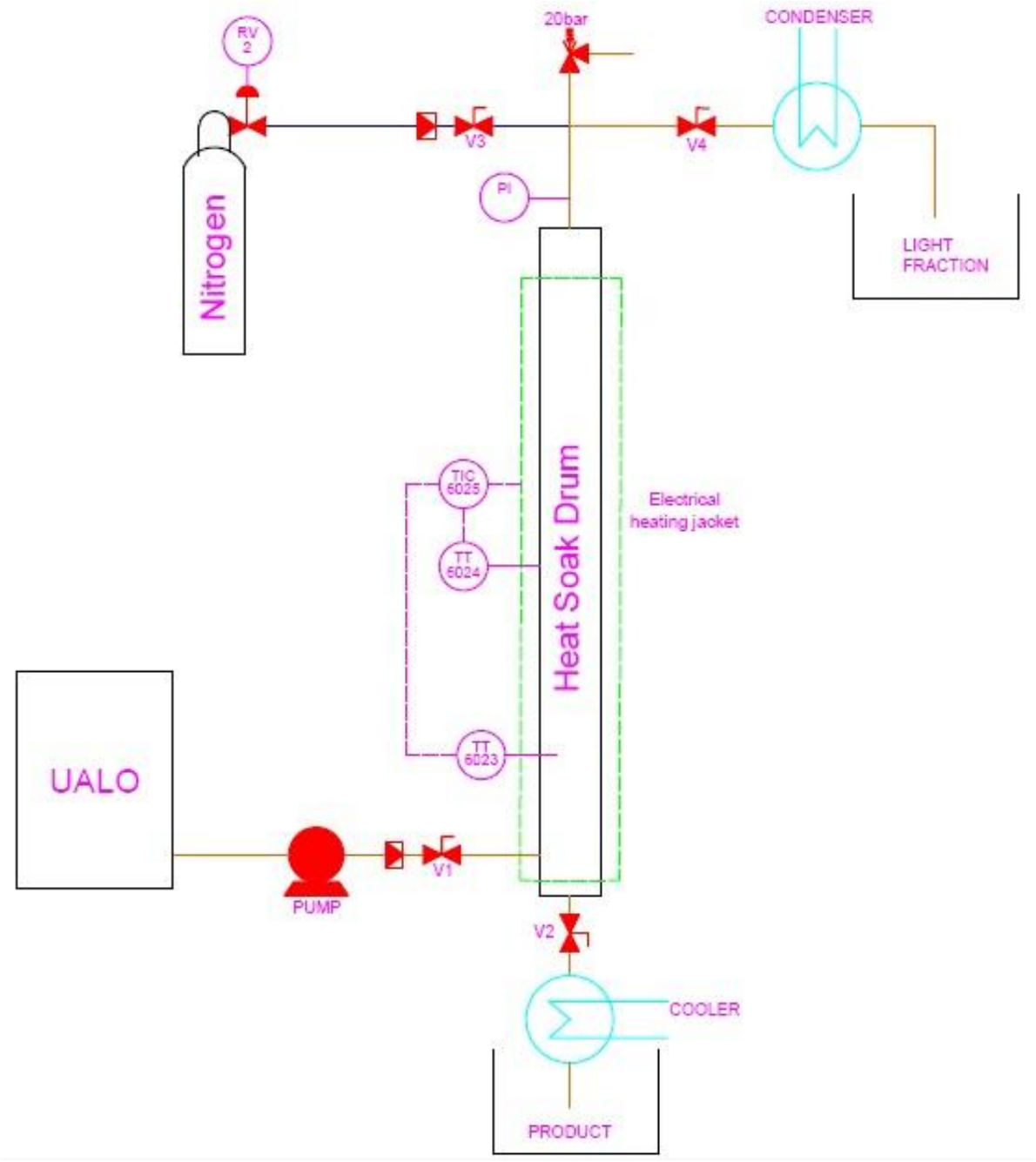

Figure 3.1 PFD of heat soak benchtop test rig

3.4.1 List of components and corresponding function (refer to figure 3.1)

a. Condenser and cooler

Function : Condenses light fractions created during the cracking process.

Description : Stainless steel coil placed in a room temperature water bath, condensation and cooling took place inside the coils.

Material of construction : Stainless steel 316L

Coil specifications : 6 m long, 4 mm ID, 6 mm OD, 150 mm coil circumference, coil element has 12 coils.

Cooling bath specification : 8” schedule 10 mild steel pipe, 300 mm long with a steel plate at the end and with a vertical orientation. It was filled with 10 L of room temperature water.

b. Pump

Function : Charges the heat soak drum with UALO at the beginning of each run.

Make : Taiver

Model : 4200

Power rating : 0.75 kW

c. Heat soak drum

Function : Contains the oil for the required residence time while thermal cracking takes place

Material of construction : Mild steel 300WA

Drum specifications : 2.5" Schedule 40 pipe, 400 mm long, 2.5" ASA 300 lb flanges, 2.5" schedule 40 end cap and 3x 3000 lb ½" sockets.

d. Electrical heating jacket

Function : Used to control the temperature inside the heat soak drum

Power rating : 3 kW (220V)

Dimensions : 300 mm X 200 mm

e. Valve V4

Function : Used to control the pressure inside the heat soak drum

Description : ½" 300 lb mild steel needle valve was used

f. Thermocouples

Type J thermocouples were used to measure the temperature of the oil inside the heat soak drum as well as the temperature of the skin on the outside of the heat soak drum. These temperatures were used to turn the heating blanket on and off via temperature controllers, thereby controlling the temperature of the oil inside of the heat soak drum at the desired set point.

g. Other

Valves : 2x ½" 300 lb mild steel gate valves were used to isolate the heat soak drum during runs.

Non-return valves : 2x ½" 300 lb mild steel non return valves were used to prevent reverse flow.

Pressure gauge : 100 mm dial, stainless steel, 0-20 bar, glycerol filled, bottom entry pressure gauge was used. A ½" pig tail was used to protect it from the high temperatures.

Safety relief valve : Brass adjustable pressure relief valve with a stainless steel ` seat.

Piping : ½" schedule 40 mild steel piping was used

3.4.2 List of materials

a. Nitrogen

Nitrogen was used to flush the system of air and to pressurise the system at the lower temperature runs.

b. UALO

UALO was the feed of which 800 mL was pumped in for each run.

3.5 Design of experiment (DOE)

Computer software called Design Expert by Statease was used to design the experiments. A central composite response surface design was used with the aim of building a quadratic model with a two level factorial experiment. The two level factorial design results in less runs required, as opposed to the one at a time factorial design. The DOE, two level factorial experiment, gave the number of runs required, 19 in total, to develop a mathematical model for optimisation of the three input variables; temperature, pressure and residence time. Optimisation was based on two responses; namely achieving the objective of producing oil with the correct viscosity in cSt at 40^{o}C and the product yield in mass %.

The central composite response surface design was selected because it is a DOE technique for the optimisation of variables and thus the process, and selecting operating conditions to meet product specification once the important variables have been first identified. The important variables and ranges are usually identified by screening designs, but in the case of this thesis, the important variables were identified through literature, namely; temperature, pressure and residence time. See Table 3.1 for the DOE experiment matrix.

Table 3.1 DOE experiment matrix

		Factor 1	Factor 2	Factor 3
Std	Random run order	A:Temperature	B:Pressure	C:Residence Time
		Deg C	bar(g)	min
15	1	350	7.5	40
12	2	350	15	40
10	3	500	7.5	40
11	4	350	0	40
8	5	500	15	60
5	6	200	0	60
7	7	200	15	60
18	8	350	7.5	40
2	9	500	0	20
9	10	200	7.5	40
4	11	500	15	20
1	12	200	0	20
14	13	350	7.5	60
3	14	200	15	20
16	15	350	7.5	40
19	16	350	7.5	40
13	17	350	7.5	20
17	18	350	7.5	40
20	19	350	7.5	40
6	20	500	0	60

3.6 Procedure

Every run utilized UALO from the same well-mixed container as to ensure reproducibility of the results and consistency of the feed. Each run was carried out using the following procedure:

- Heat soak drum was flushed with nitrogen
- Heat soak drum was pressurised to the required pressure with nitrogen
- Heat soak drum was heater to the required run temperature
- 800 mL of UALO was pumped into the heat soak drum
- Oil was held at the required run temperature and pressure for the required run residence time

- Product was discharged through the cooler after the expiration of the required residence time
- Light fraction (if produced) was collected and added back into final product sample
- Sample was taken to lab and analyse for viscosity and yield

3.7 Sample testing method

American society for testing and materials (ASTM) methods were used for all lab tests conducted. See table 3.2 for tests carried out and corresponding ASTM method used.

Table 3.2 Lab test and apparatus

Test	Apparatus	ASTM Method
Viscosity	· Viscosity bath · Viscosity tube · Stop watch	D445
Flash Point	· Closed cup instrument	D93
Distillation	· Heating mantle · Round bottom flask · Condenser · Vacuum pump	D1160-03
Calorific value	· Calorific bomb apparatus	D240
Ash	· Crucible · Mass balance · furnace	D482

3.7.1 ASTM method D445 Viscosity test

The time was measured for a fixed volume of UALO to flow under gravity through the capillary of a number 5 calibrated viscometer with a constant of 0.3195 cSt/s under a reproducible driving head and under a closely controlled and known temperature (40^{o}C). The UALO was injected into the viscometer and placed into the pre-heated 40^{o}C water bath. This was confirmed by two independent thermocouples. The viscometer was left in the bath for 30 minutes to allow the UALO to reach 40^{o}C. The plug was then removed from the opposite end of the viscometer. The time taken for the UALO to flow between the two points on the viscometer in seconds was multiplied by the viscometer constant to give the viscosity of UALO in centistokes at 40^{o}C. See Figure 3.2 for apparatus setup.

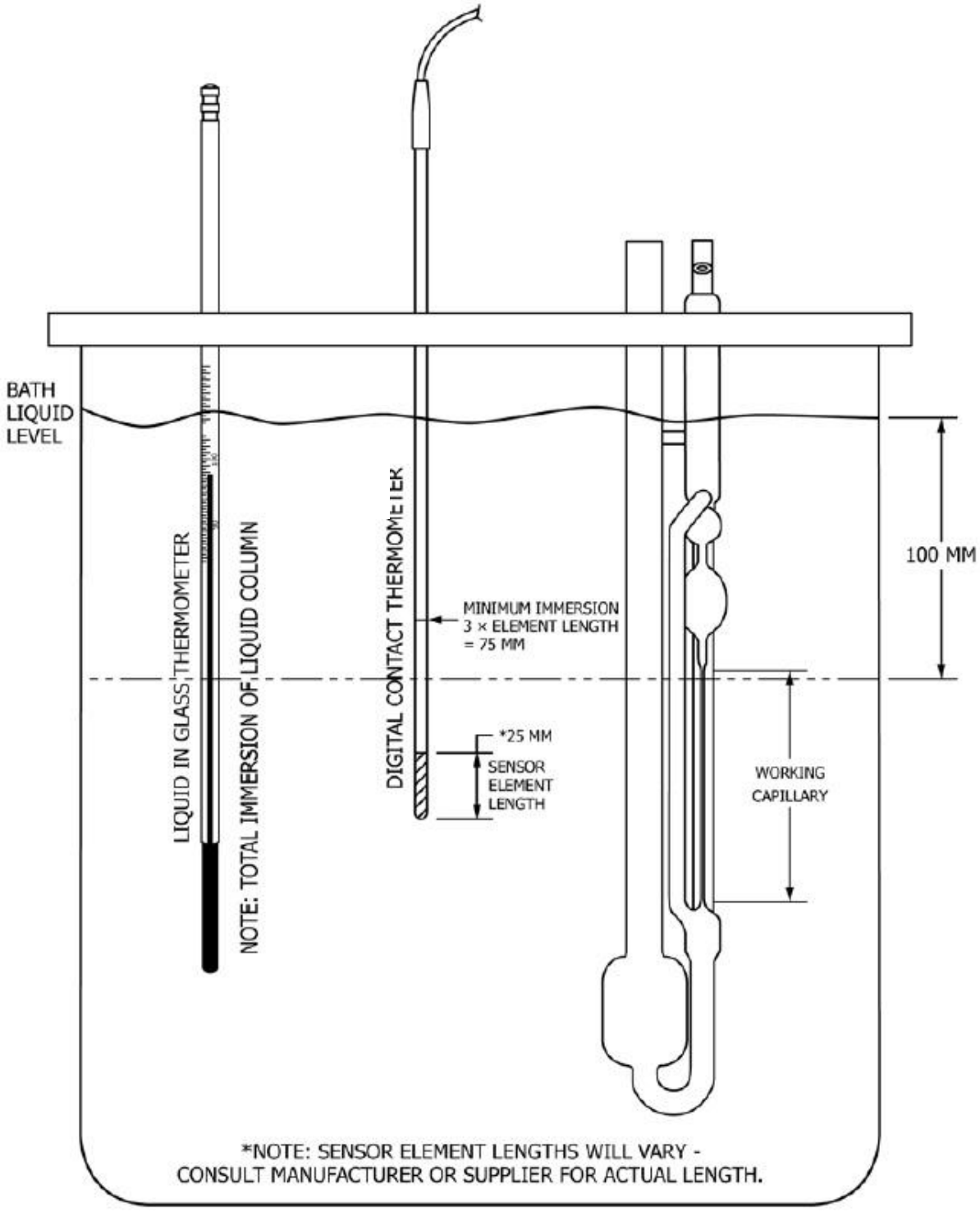

Figure 3.2 Reverse flow viscometer apparatus (ASTM D445)

3.7.2 ASTM method D93 Flash Point test

The flash point was tested by adding 75 mL of UALO into an automated Pensky-Martens closed cup apparatus. The stirrer was set at 120 rpm and oil heated at a rate of 5^{o}C/min. The flash point was tested at 45^{o}C by stopping the stirring and opening the hatch and exposing the vapour space above the oil to an open flame for 0.5 seconds. The same was done at 50^{o}C. When the vapour space failed to ignite at both temperatures, the flash point of the UALO was said to be above 50^{o}C. See Figure 3.3 for the assembly drawing of the Pensky-Martens closed cup apparatus.

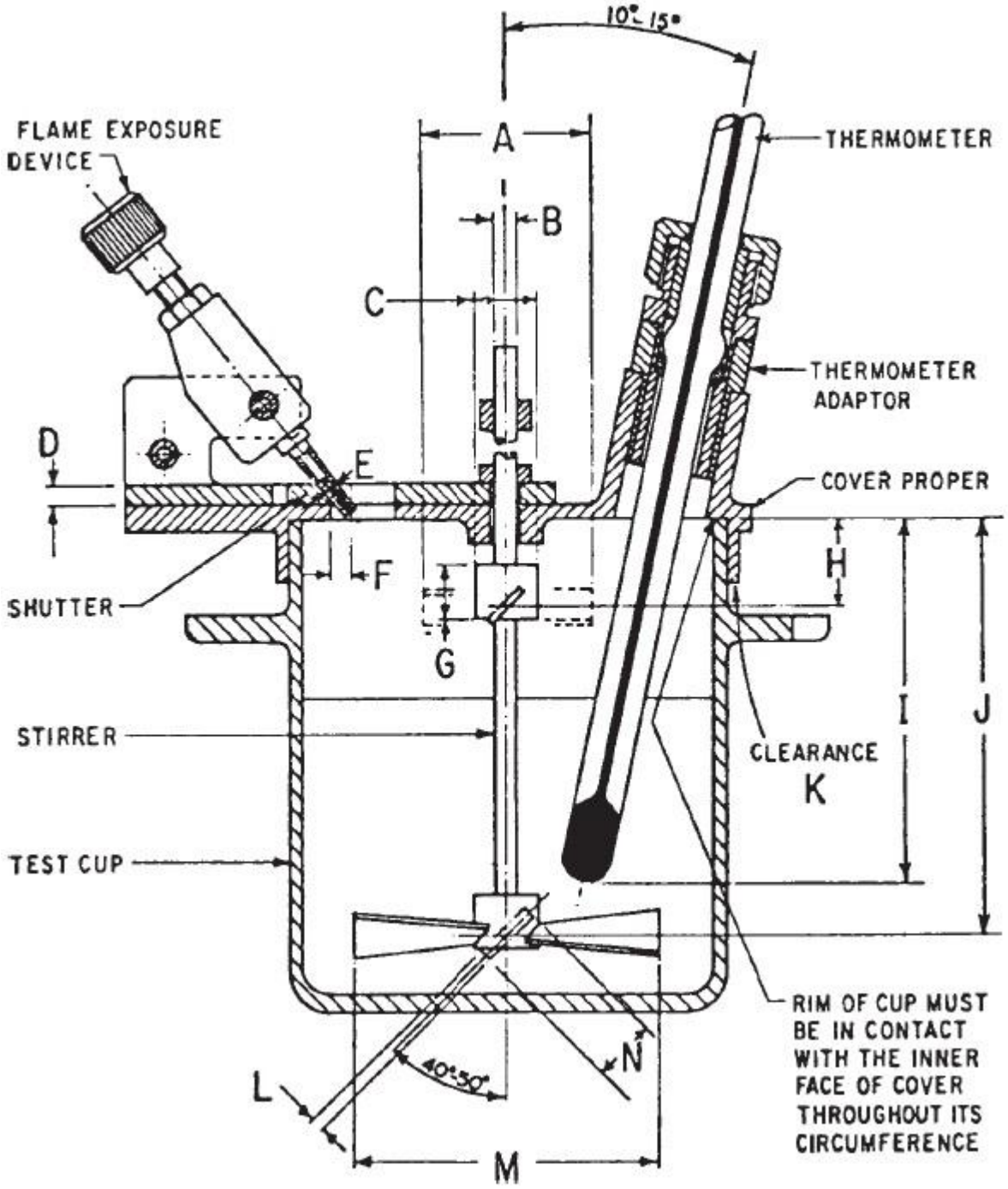

Figure 3.3 Pensky-Martens Closed Cup Apparatus (ASTM D93-02)

3.7.3 ASTM method D1160-03 Vacuum Distillation

All UALO product samples were ditilled under vacuum conditions using the apparatus depicted in Figure 3.4.

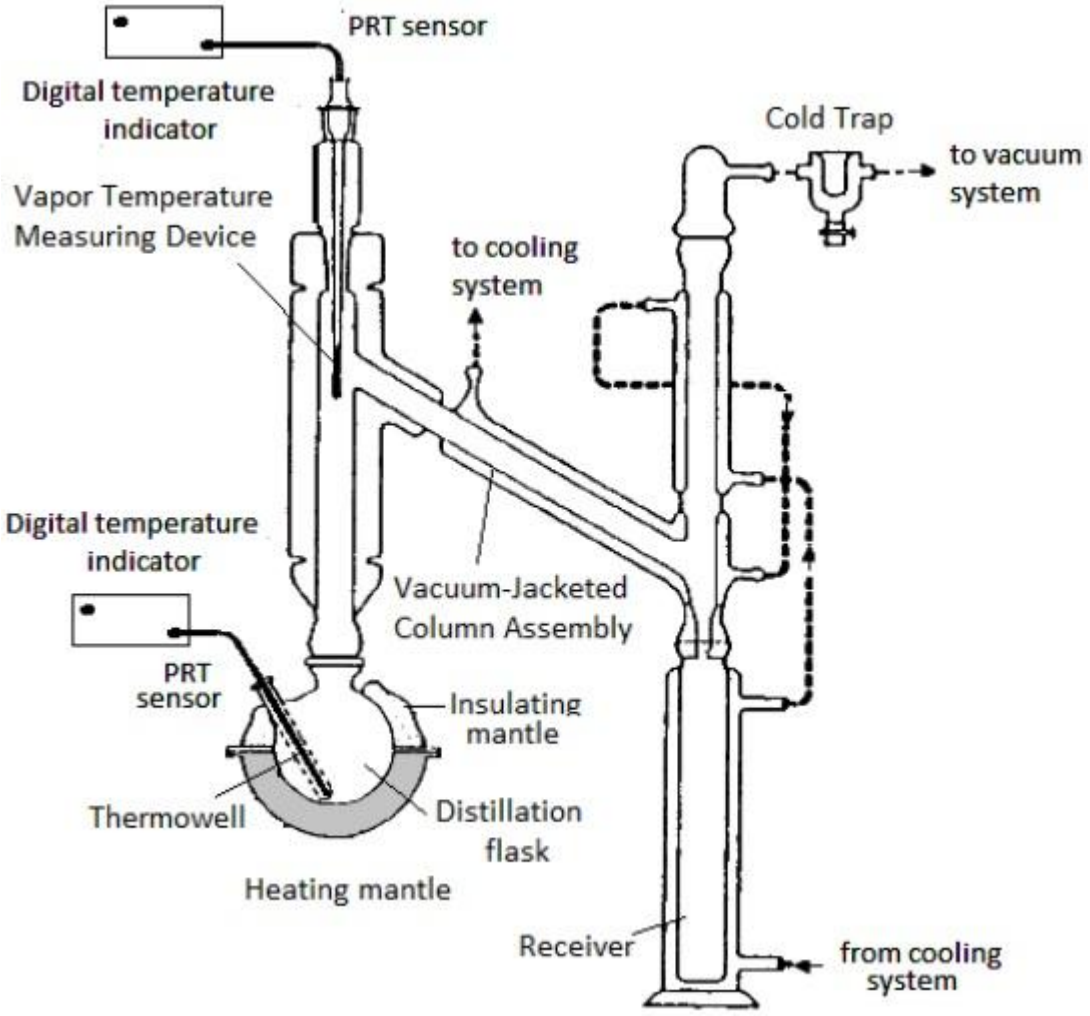

Figure 3.4 Vacuum distillation apparatus (ASTM D1160-03)

100 g of sample was added into the round bottom flask and a high vacuum was drawn < 10 mbar. Heating was started and the distillate was condensed in the condenser using the cooling water and collected. The amount of distillate distilled off along with the associated pressure and temperature was recorded. Vacuum distillation was used to prevent any further cracking of the UALO.

3.7.4 ASTM method D240 calorific value test

The calorific value of the UALO product was tested in a Bomb Calorimeter. In each test 0.6 g of oil was placed into the bomb calorimeter and the bomb calorimeter charged with 30 atmospheres of oxygen. The temperature was allowed to stabilise before the instrument

ignited the oil and measured the associated temperature rise. The instrument used the inputted mass of the sample and the associated temperature rise from its combustion in calculating the calorific value of the oil sample in MJ/kg.

3.7.5 ASTM method D482 ash test

The ash content of each sample was tested by weighing an empty crucible to the nearest 0.0001 g. Approximately 20 g of oil was added to the crucible before it was re-weighed to the nearest 0.0001 g. The oil was burnt off using a Bunsen burner before being placed in a furnace at 800^{o}C for 5 hours, burning off all remaining carbon, leaving just the ash that was contained in the oil. The crucible was then removed and placed in a desiccator to cool. After the crucible had reached room temperature, it was re-weighed to the nearest 0.0001 g. The percentage ash was calculated using the following equation.

$$\%ash = \frac{mass\ of\ cool\ crucible\ after\ furnace - mass\ of\ empty\ crucible}{mass\ of\ cool\ crucible\ with\ oil - mass\ of\ empty\ crucible} X100$$

See Table 3.3 shows the feed specifications and the corresponding required product specifications

Table 3.3 Feed and product specifications

Property	**Feed (value)**	**Product (LO10 spec)**
Viscosity @ 40^{o}C (cSt)	43 - 48	8-10
Flash point (^{o}C)	75 - 90	> 50
Calorific value (GJ/ton)	44	>44
Ash content (wt%)	0.8-1.2	<0.08

a. Viscosity

The viscosity was determined at 40^{o}C using ASTM method D445 and inputed as a response in the response surface model to develop a mathematical model describing the effect that temperature, pressure and residence time has on the viscosity of UALO.

b. Flash point

The flash point was used to determine whether or not the >90% yield was met. See Yield test for more information.

c. Distillation

Vacuum distillation was carried out on the feed samples as well as all the product samples. All product distillation curves were compared to that of the feed to ascertain the degree of cracking that occurred at the various process conditions laid out by the DOE. The distillation was carried out under vacuum and the curve later corrected to atmospheric pressure using a nomograph. The pressure-temperature nomograph can be found in appendix D.

d. Yield test

The gas make and sludge formation was found to be negligible, therefore the yield was determined by distilling off 10% of the product and then testing the flash point of the bottom 90%. If the flash point of the bottoms (remaining 90%) was found to be >50^{o}C (LO10 flash point specification), then the liquid yield was said to be >90%.

e. Additive package test

A drop test was employed to test whether or not each respective run destroyed the additive package present in UALO. A drop test consists of dropping a drop of oil onto a filter paper and then observing the outcome. The additive package was considered destroyed when the soot present in the oil stayed in the centre of the drop and the oil diffused through the paper. This resulted in a golden brown circle with a smaller black circle in the centre. If the soot diffused with the oil, the additive package had not been broken down; this resulted in one black circle with a small golden brown edge (figure 3.5). However the drop test did not prove

to be reliable in terms of indicating when the additive package had been broken down. Appendix C, shows that there is no clear trend in the drop test results. A settling test was instead adopted, where samples were left to settle for one week and the tops tested for ash. Low ash results indicate that the additive package had been broken.

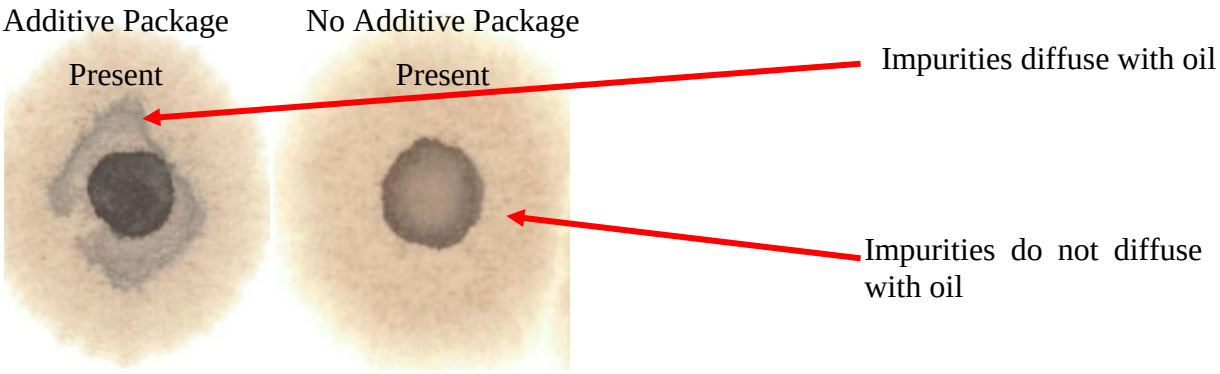

Figure 3.5 Example of oil drop test

f. Calorific value test

The calorific value was determined with a bomb calorimeter using the ASTM D240 method. The calorific value is required to ensure that the fuel meets the energy requirements for economic purposes because a low calorific value means that more fuel needs to be burnt.

g. Ash test

The ash content of the fuel was determined via a five hour ash test following ASTM method D482. The ash content of the fuel in mass % indicates the amount of metals present. A high metal concentration in fuels leads to the rapid fouling of boilers, ovens and furnaces, thereby increasing running cost.

3.8 Data analysis

A total of three runs were carried out for each set of process conditions required by the DOE. These three runs were used to establish repeatability and significance of the data. The data set was deemed to be significant when the coefficient of variation was less than 5% (Madelon, 1999). Once statistical significance had been established, the mean viscosities and yields of each data set were inputted into Design Expert and a mathematical model was produced. The regression coefficient was checked and found to be below 0.95. Data transformation was attempted at first followed by a change in the design model (curve fitting).

3.9 Optimum conditions

The model developed through experimentation was used to identify the optimum operating conditions. The optimum values being the minimum values of temperature, pressure and residence time at which the bench top test rig converts UALO to LO10 with all specifications being met. Three runs were carried out at the models outputted optimum operation conditions and the three resulting runs were found to have met all of the LO10 specifications, and the viscosities were all within a 5% relative error. The optimum operating conditions therefore were deemed to be statistically significant and the conditions were accepted.

3.10 Research limitations

The methodology used a common UALO feed collected from a bulk storage tank for all experimentation and due to this, the model developed from the results may not be valid for other UALO feed stocks. Further work will need to be carried out to assess the validity of the model with respect to other UALO feed stocks. Additionally, the model is only valid for the variable ranges investigated.

4 Results and Discussion

4.1 Introduction

This section presents the results of the thesis and discusses the findings in detail. The chapter begins with presenting the average of three runs for each trial, for both viscosity and yield, along with the verification of the viscosity response statistical significance. It continues with the development of the UALO heat soak model, and its confirmation. Gaps in the findings are discussed. The chapter closes with summarising the answers to the research questions.

4.2 Qualitative results

The literature review conducted on refinery processes revealed a number of existing as well as emerging technologies capable of reducing the viscosity of heavy feed stocks. The in depth review of UALOs physical and chemical properties revealed thermal cracking to be preferred process for breaking the additive package in UALO and reducing its viscosity while maintaining sufficiently high yields (>90%) (Green & Wittcoff, 2008). The additive package in UALO starts breaking down at temperatures in excess of 200^{o}C (Nora Corporation, 2003) and thermal cracking employs high temperatures >350^{o}C to crack and reduce the viscosity of heavy oil. This cracking takes place via the free radical mechanism (Clark, 2003).

The asphaltene micelles present in UALO are also disturbed at these high temperatures, causing the asphaltene particles to agglomerate and drop out of suspension, along with the high ash content and viscosity associated with asphaltenes (Sieli, 1998). The three most important properties of thermal cracking are temperature, pressure and residence time (Sieli,1998; Speight, 2008).

Catalytic cracking was also found to be capable of reducing the viscosity and breaking the additive package of UALO by employing high temperatures in the presence of a catalyst, but at a higher selectivity via the catalytic cracking mechanism (Sadighi & Mohaddecy, 2013; Wilczura-Wachnik, 2009). However, catalytic cracking produces a large amount of gas >10% (Goncharov & Belyaevskii, 2005), therefore making it undesirable in terms of the aim of this work; producing valorised LO10 with a lquid yield greater than 90%.

Additionally, the high content of impurities such as asphaltenes found in UALO renders the use of a catalyst impractical, as rapid fouling would result. Catalytic cracking is therefore not a viable option, rendering thermal cracking as the logical choice.

The two main types of thermal cracking found in industry today are visbreaking and delayed coking. Delayed coking produces large amounts of coke and gas, as much as 10 – 30%, where visbreaking produces approximately 8% gas and a negligible amount of coke (Stratiev et al., 2008). It was for this reason that visbreaking was selected over delayed coking.

Literature describes two well documented types of visbreaking processes. The coil type which operates at temperatures and residence times of 500^{o}C and 3 min (time in coil) respectively, giving run lengths of 3-6 months before the coil needs to be de-coked. The second is the heat soak drum type which operates at temperatures and residence times of 443^{o}C and 30 minutes (time in drum) respectively, giving run lengths of 6-18 months before the coil needs to be de-coked (Agorreta et al., 2011); the heat soak drum type was adopted because the reduced residence time (1-2 seconds) in the heating coil results in longer runs before de-coking is required (Mohaddecy, Sadighi, Ghabuli & Rashidzadeh, 2011).

The coil design is an intricate part of the process (Robinson, 2007) in terms of heating and run length, but does not contribute significantly to the degree of cracking in the drum type visbreaking unit (Sepehr & Moheddecy, 2013). Therefore in terms of the scope of this thesis, only the conditions in the heat soak drum was investigated. A heat soak drum bench top test rig was designed and set up in order to conduct the quantitative part of this thesis.

4.3 Quantitative results

The average results for the trials can be viewed in Table 4.1. The resulting average viscosity for each trial had a coefficient of variance well below 5% which is indicative of statistical significance (Madelon Zady,1999); they were therefore used to develop the UALO heat soak model. Ten percent by mass was distilled off from samples from each run and the flashpoint tested. The flash point for each sample tested was found to be above 50^{o}C therefore no additional distillation was required to correct the flash point. Additionally, the coke and gas production was negligible therefore it can be said that the final liquid product yield for each run was above 90%. It was therefore decided to exclude the yield from the model as it would not form part of any constraint.

The following describes the viscosity reduction seen in Table 4.1. The asphaltenes and additives such as the viscosity modifier in UALO contribute toward viscosity (Badger & Harold, 2001). Shaw (1992) found that the asphaltenes agglomerate and drop out at high temperature due to the breakdown of the micelles. The Nora Corporation (2003) found that the UALO additive package breaks down at temperatures above 200^{o}C (Nora Corporation, 2003). It is therefore likely that the viscosity reduction seen at the lower temperatures 200-300^{o}C was from the additive package breakdown and asphaltene dropout.

The reduction in viscosity at temperatures above 350^{o}C can be attributed to thermal cracking via the free radical mechanism. The free radical mechanism works at temperatures above 350^{o}C (Green & Wittcoff, 2008). This mechanism consists of three steps; first the high temperature created a small amount of free radicals. Secondly, the free radicals reacted with other molecules by cracking them hence producing shorter molecules and more free radicals through propagation. Thirdly, the free radicals reacted with each other and to a lesser extent with the reactor walls and terminated (Angeira, 2008). As the temperature increased, more free radicals were produced resulting in a higher degree of cracking and as a result a lighter, lower viscosity product was produced.

Table 4.1 Results: Viscosity response

	Factor 1	Factor 2	Factor 3	Response 1		Response 2
Random trial order	A:Temperature (Deg C)	B:Pressure (barg)	C:Residence time (min)	Viscosity Average of 3 runs (cSt)	Coefficient of variation (%)	Yield Average of 3 runs (%)
1	350	7.5	40	39.78	1.09	> 90
2	350	15	40	38.23	0.88	> 90
3	500	7.5	40	13.69	1.03	> 90
4	350	0	40	40.84	0.74	> 90
5	500	15	60	7.08	0.98	> 90
6	200	0	60	50.83	0.20	> 90
7	200	15	60	50.35	0.75	> 90
8	350	7.5	40	39.48	1.33	> 90
9	500	0	20	26.05	2.38	> 90
10	200	7.5	40	51.40	1.81	> 90
11	500	15	20	22.23	0.60	> 90
12	200	0	20	53.41	0.47	> 90
13	350	7.5	60	32.69	2.93	> 90
14	200	15	20	52.41	0.42	> 90
15	350	7.5	40	40.02	0.87	> 90
16	350	7.5	40	39.10	0.29	> 90
17	350	7.5	20	45.38	0.92	> 90
18	350	7.5	40	39.85	0.77	> 90
19	350	7.5	40	38.46	1.62	> 90
20	500	0	60	7.72	3.51	> 90

4.3.1 Model results & statistical analysis

The mean viscosity response in Table 4.1 was inputted into the design expert and a square root transformation used to yield an adjusted R-squared and predicted R-squared of 0.998 and 0.992 respectively (*refer to Table 4.2)* with a quadratic curve fit, meaning that it was a good fit for the data and that the correct amount of variables were used in developing the model. The high predicted R-square value means that the model will predict future results accurately. The cubic curve fit had the higher adjusted R-squared 0.999 but was rejected because of the poor predicted R-squared 0.804 value, meaning that the model would poorly predict future results. This however is not always an indication of predictiability.

Table 4.2 Model selected

Source	Adjusted R-Squared	Predicted R-Squared	
Linear	0.835	0.730	
2FI	0.879	0.530	
Quadratic	0.998	0.992	Selected
Cubic	0.999	0.804	

Note all models above have undergone a square root transformation

The statistical analysis showed that the experimental data is repeatable and reliable, and that a quadratic model with a square root transformation can be used to accurately predict future viscosity values for temperature, pressure and residence time ranges of 200-500^{o}C, 0-15 bar (g), and 20-60 min respectively. The terms and coefficients of the model can be viewed in Table 4.3.

Table 4.3 Model (square root transformation)

Constants	Factor
4.673478903	(constant)
0.02077461	* Temperature
-0.018345008	* Pressure
0.030892632	* Residence T
-4.49144E-05	* Temperature * Pressure
-0.000169045	* Temperature * Residence T
0.000255321	* Pressure * Residence T
-3.57126E-05	* Temperature^2
0.00086413	* Pressure^2
-2.8075E-05	* Residence T^2

4.3.2 Equation generated from model

The equation for the model is as follows

$$\upsilon = \left[\left(\begin{matrix}-0.0357126T^2 + 0.86413P^2 - 0.028075\tau^2 + 0.255321PR - 0.169045T\tau \\ -0.0449144TP + 20.77461T - 18.345008P + 30.892632\tau + 4673.47890\end{matrix}\right)/1000\right]^2 \quad --(14)$$

Where:

υ : Viscosity @ 40°C in cSt

T : Temperature in degrees Celcius

P : Pressure in bar (gauge)

τ : Residence time in minutes

The coefficients in the model are extremely small but are significant in terms of the end result due to the magnitude of the variables that they are being multiplied by. The sensitivity analysis in Table 4.4 clearly indicates that all terms are necessary for an accurate viscosity prediction. 6 different combinations of the equation were tried each time leaving out different terms. Equation 14 is the original equation with no changes and equations 15, 16, 17, 18 & 19 are the equations with different combinations of terms.

Table 4.4 Sensitivity analysis on developed model

Input Variables			Viscosity @ 40Deg C (cSt)					
Temperature (Deg C)	Pressure (barg)	Residence Time (min)	Equation 14	Equation 15	Equation 16	Equation 17	Equation 18	Equation 19
200	5	30	52.03	93.38	10.51	40.20	20.78	20.80
250	5	30	51.61	114.54	5.94	39.83	20.68	18.55
300	10	20	49.38	128.60	2.35	42.81	19.73	18.20
350	10	40	38.40	168.92	0.12	25.46	19.53	12.23
400	15	60	22.38	212.04	0.90	8.66	18.69	5.61
500	15	45	10.68	261.66	16.95	3.97	18.11	4.85

$$\upsilon = \left[\left(\begin{matrix}-0.0357126T^2 + 0.86413P^2 - 0.028075\tau^2 + 0.255321PR - 0.169045T\tau \\ -0.0449144TP + 20.77461T - 18.345008P + 30.892632\tau + 4673.47890\end{matrix}\right)/1000\right]^2 \quad --(14)$$

$$\upsilon = [(20.77461T - 18.345008P + 30.892632\tau + 4673.47890)/1000]^2 - -(15)$$

$$\upsilon = [(-0.0357126T^2 + 0.86413P^2 - 0.028075R\tau^2 + 4673.47890)/1000]^2 - -(16)$$

$$\upsilon = [(-0.0357126T^2 - 0.169045T\tau - 0.0449144TP + 20.77461T + 4673.47890)/1000]^2 - -(17)$$

$$\upsilon = [(0.86413P^2 - 0.0449144TP - 18.345008P + 4673.47890)/1000]^2 - -(18)$$

$$\upsilon = [(-0.028075\tau^2 - 0.169045T\tau + 30.892632\tau + 4673.47890)/1000]^2 - -(19)$$

Equations 15 through 19 where different combinations of selected terms were left out resulted in vastly different results to that of equation 14 (seen in Table 4.4). These equations (15-19) are therefore inaccurate at predicting the viscosity, confirming that all terms in equation 14 are significant.

4.4 Model confirmation

A confirmation test was carried out to test the results of the statistical analysis and thereby validate the model (refer to Table 4.5 and Figure 4.5). The measured viscosities of the 6 random confirmation runs all matched the models predicted viscosities within a 5% relative error. Based on the accuracy confirmation of the model, it was used to determine the conditions within the relevant ranges at which the resulting product would meet the LO10 viscosity specifications of 10 cSt at 40^{o}C. An "optimum" run was carried out and the resulting viscosity was compared to the predicted viscosity. It was also found to be within a 5% relative error. The optimisation run therefore served as a 7th confirmation run for the model. Looking at Table 4.5 and Figure 4.5 it can be seen that the % relative error increased as the resulting viscosity decreased. This could be attributed to some error involved in the analysis of the viscosities in the laboratory.

Table 4.5 Model confirmation

	Factor 1	Factor 2	Factor 3	Response		
Confirmation run	A:Temperature (Deg C)	B:Pressure (barg)	C:Residence time (min)	Predicted viscosity (cSt)	Measured viscosity (cSt)	% Relative Error
1A	200	0	45	52.01	51.73	0.54
2A	300	5	30	48.62	48.45	0.35
3A	320	10	60	37.01	36.84	0.46
4A	350	12	60	32.17	31.99	0.56
5A	400	15	30	34.9	34.43	1.37
6A	500	15	45	11.04	10.61	4.09
Optimum (7A)	475	15	60	9.95	9.51	4.66

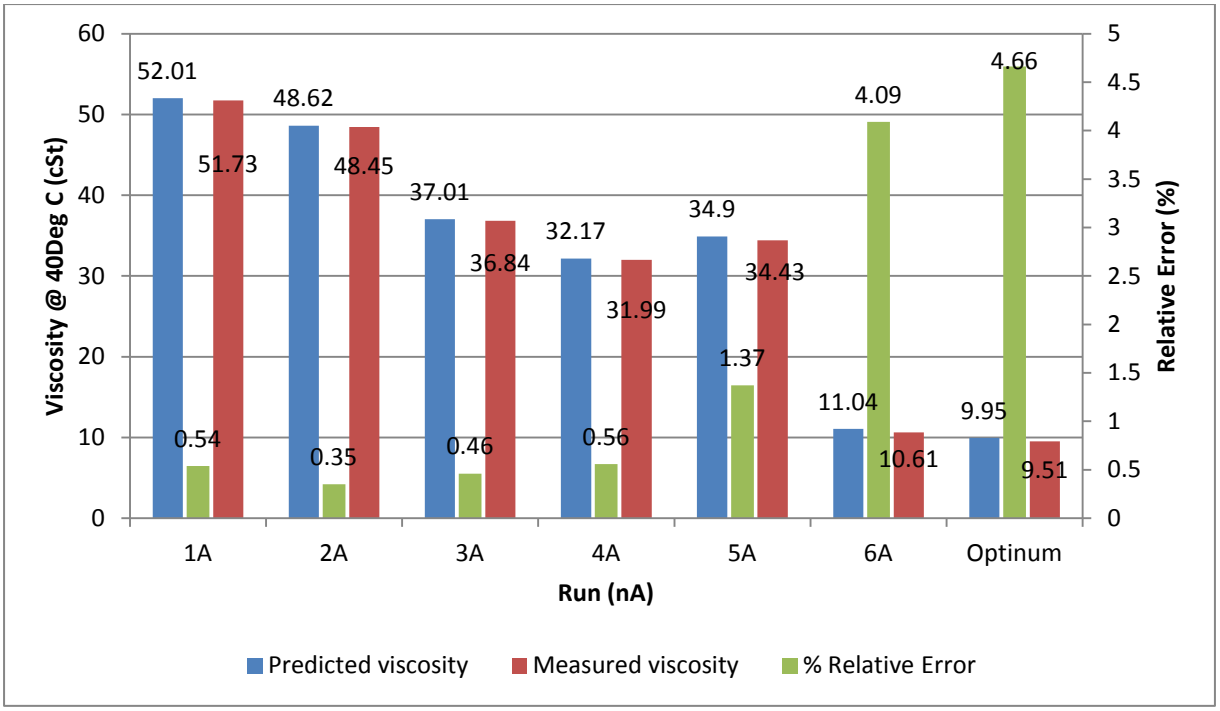

Figure 4.1 Predicted viscosity vs measured viscosity

$$\%\ relative\ error = ((predicted\ value - actual\ value)/actual\ value)\ X\ 100 - -(20)$$

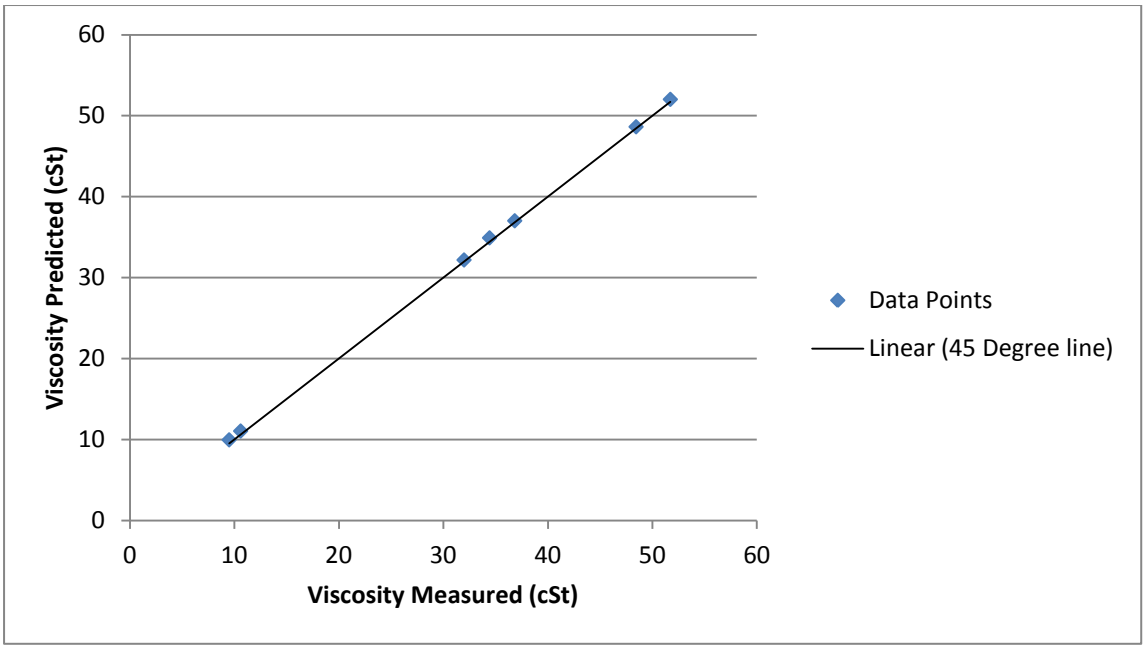

Figure 4.2 Data fit (7 confirmation runs and model)

The data points of predicted viscosity vs measured viscosity in Figure 4.2 lie very close or on the 45 degree line,the further indicating the accuracy of the model. However, in table 4.5

and figure 4.1 it can be seen that the model although accurate at predicting the viscosity of each random run is consistently over-predicting. This over-prediction may have originated from a new constant error in either one of the measuring instruments in the bench top test rig or laboratory apparatus. The values of the over prediction can be seen in Table 4.6.

Table 4.6 Confirmation run over prediction

Confirmation run	Absolute error (cSt)	Measured viscosity (cSt)	Predicted viscosity (cSt)	New predicted viscosity (cSt)	New absolute error (cSt)	New relative error %
1A	0.28	51.73	52.01	51.73	0.00	0.00
2A	0.17	48.45	48.62	48.34	-0.11	-0.23
3A	0.17	36.84	37.01	36.73	-0.11	-0.30
4A	0.18	31.99	32.17	31.89	-0.10	-0.31
5A	0.47	34.43	34.9	34.62	0.19	0.55
6A	0.43	10.61	11.04	10.76	15	1.45
Optimum (7A)	0.44	9.51	9.95	9.67	0.16	1.72
Average	0.3				0.03	

$$absolute\ error = \ predicted\ value - actual\ value - -(21)$$

The absolute error values in Table 4.6 can all be seen to be positive. The average absolute error was calculated to be 0.28cSt. This average absolute error was subtracted from each of the predicted values to give a new predicted value for each of the confirmation runs. The new average absolute error is 0.03 which indicates a better spread. This predicted transformation significantly lowered the relative errors as expected. Both the old and the new predicted values for the optimum run lie within the viscosity specification of LO10.

The graphic representation of the model equation can be seen in Figures 4.3, 4.4 and 4.5. Figure 4.3 is a three dimensional surface plot of viscosity-pressure-temperature for the optimum residence time of 60 min. Figure 4.4 is a three dimensional surface plot of viscosity-pressure-residence time for the optimum temperature of 475^{o}C. Figure 4.5 is a three dimensional surface plot of viscosity-temperature-residence time for the optimum pressure of 15 bar(g).

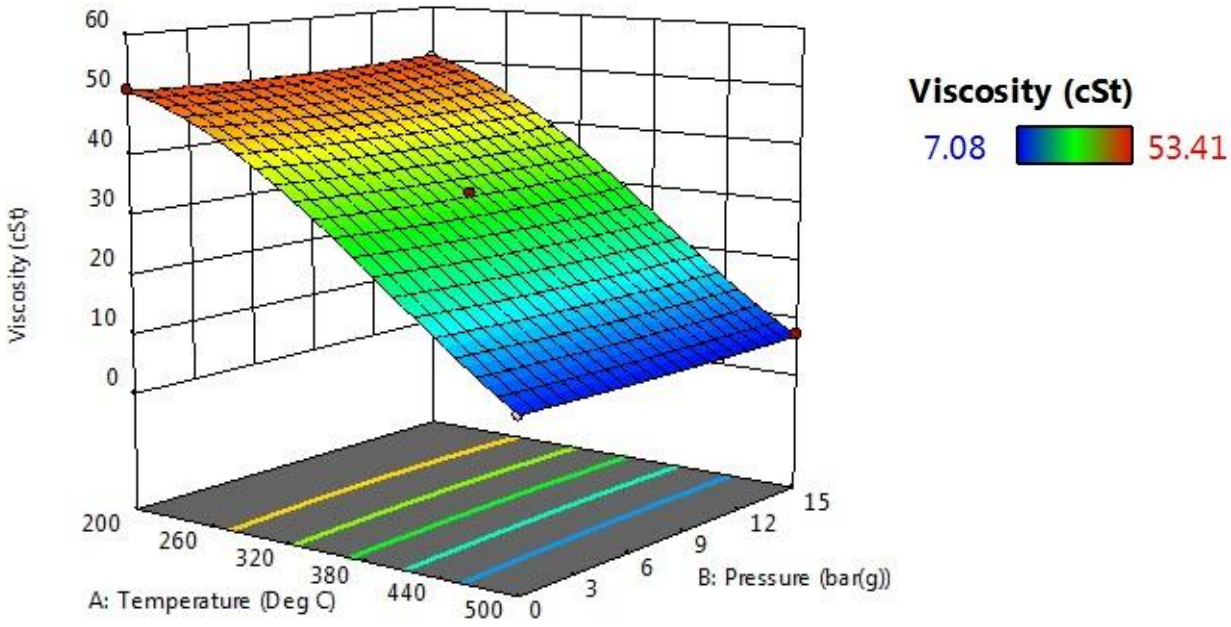

Figure 4.3 Three dimentional surface plot of viscosity-temperature-pressure

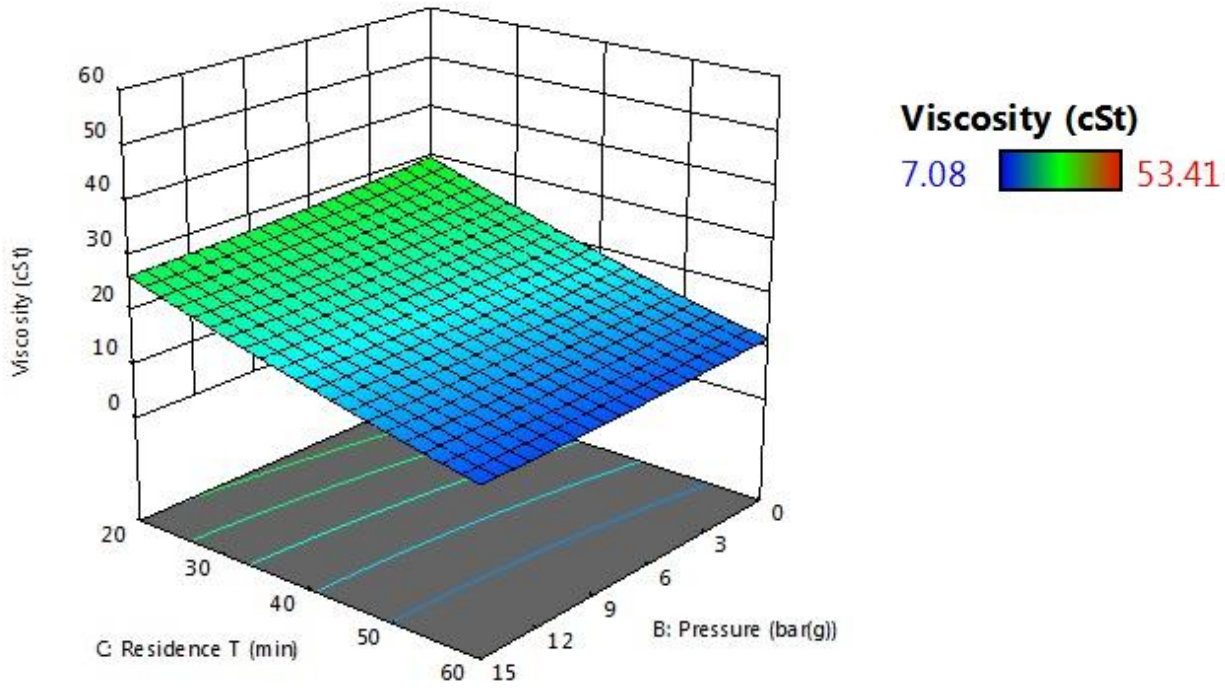

Figure 4.4 Three dimentional surface plot of viscosity-pressure-residence time

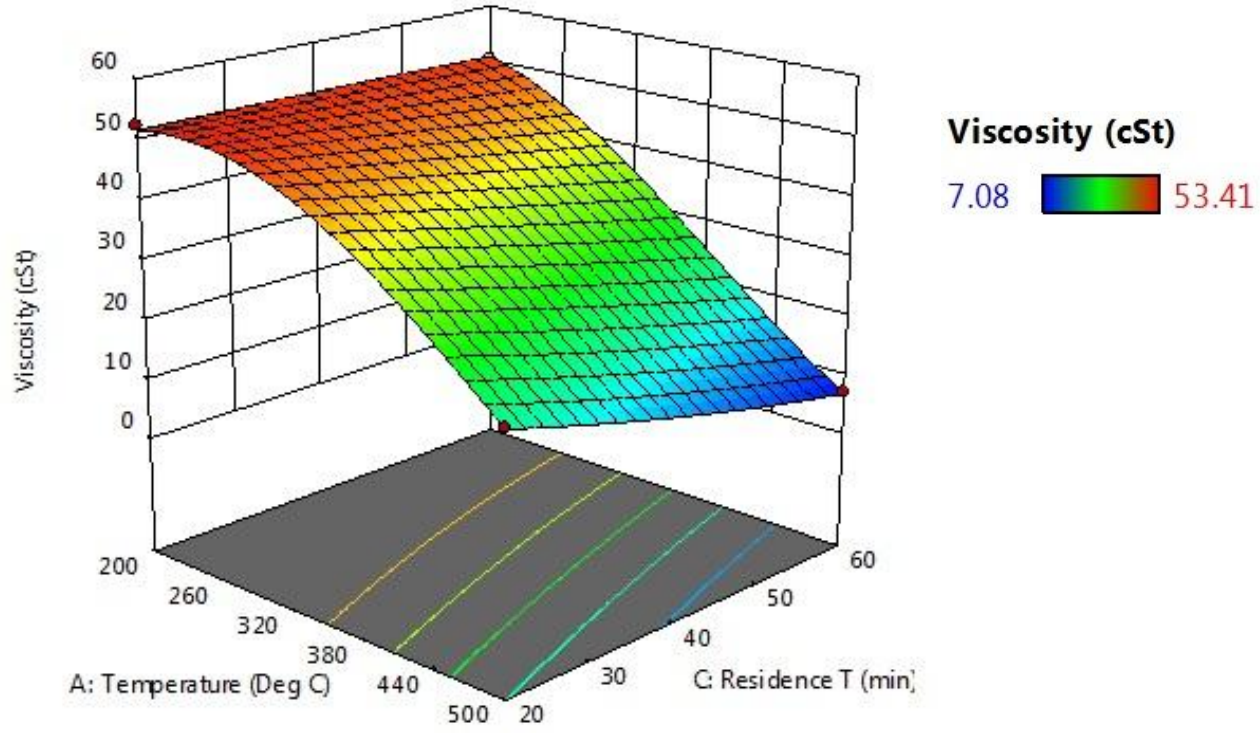

Figure 4.5 Three dimentional surface plot of viscosity-temperature-residence time

4.5 Degree of cracking

The distillation data for the confirmation runs can be viewed in Figure 4.6. The distillation data reveals clear evidence of cracking through all the runs, from the minimum temperature of 200^{o}C through to the maximum temperature of 500^{o}C. This was evident by the fact that larger fractions were distilled off at lower temperatures when compared to the feed. It is well known that when large molecules crack, they form smaller molecules with lower boiling points (Green & Wittcoff, 2006).

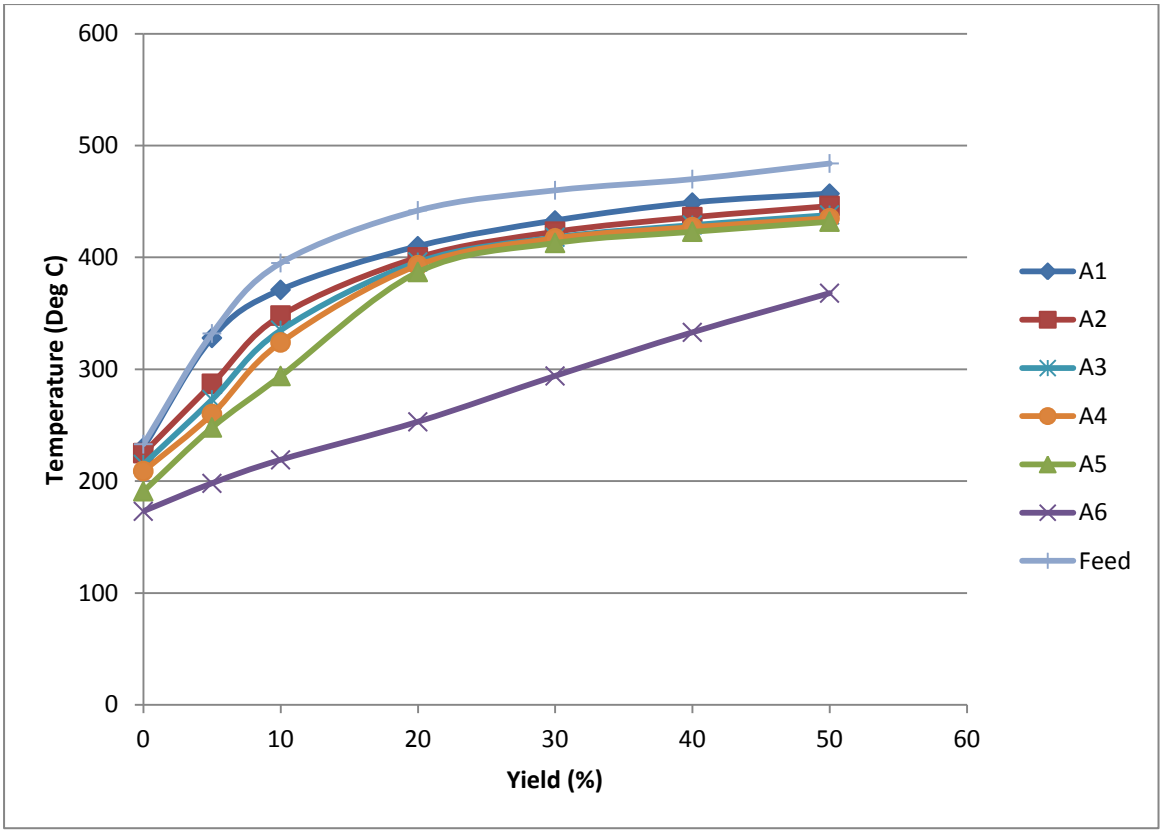

Figure 4.6 Distillation curves

In Figure 4.6 the distillation curves of the product for each of the confirmation visbreaking runs can be observed. The distillation curves represent the boiling range of the first 50% by mass of oil distilled off of the product of each of the runs.

It can clearly be seen from figure 4.6 that the higher temperature 500^{o}C visbreaking run in A6 had a far greater effect on reducing the boiling point range and therefore bringing the molecular size distribution of the UALO closer together. Compare the boiling point range/curve of run A6 with that of run A1 and the feed. The difference is clear, the higher the visbreaking temperature, the higher the degree of cracking, evident by the lower boiling point range of run A6. This finding is supported by literature (Green & Wittcoff, 2006). Additionally it can be seen that the shape of the boiling point curve of the lower temperature visbreaking runs <=400^{o}C had a similar shape to the boiling point curve of the feed, where the 500^{o}C visbreaking temperature run in A6 has a vastly different shape, indicating that the heavy molecules have broken down to a greater extent at the higher temperatures resulting in the heavier components boiling point range between the 20-50% distillation point being 125^{o}C and lighter components having a lower boiling point range between the 0-20%

distillation point of 75^{o}C. Compare this to the lower temperature runs where the heavier components boiling point range between the 20-50% distillation point was lower at 50^{o}C and the lighter components having a higher boiling point range between the 0-20% distillation point of 200^{o}C. The lower boiling point range on the lighter components in run A6 indicates that some oil was lost as gas. The breakdown of the additive package could also have had a limited effect on the boiling point curve due to boiling point elevation created by their presence.

4.6 Additive package

The additive package starts to break down at temperatures above 200^{o}C (Nora Corporation, 2003). Table 4.7 illustrates that as the temperature increased, the degree to which the additive package breaks down increased until a temperature was reached where no additive package remained. This was found to occur at 350^{o}C. The 3 optimum run samples were taken and left to settle over a 1 week period. The ash of the top of each of the 3 samples were tested and found to be all below 0.01%.

Table 4.7 Additive package test

	Factor 1	Factor 2	Factor 3	additive package test
Random trial order	A:Temperature (Deg C)	B:Pressure (barg)	C:Residence time (min)	Ash (%) (average of three runs)
1	350	7.5	40	<0.01
2	350	15	40	<0.01
3	500	7.5	40	<0.01
4	350	0	40	<0.01
5	500	15	60	<0.01
6	200	0	60	0.9
7	200	15	60	0.88
8	350	7.5	40	<0.01
9	500	0	20	<0.01
10	200	7.5	40	0.93
11	500	15	20	<0.01
12	200	0	20	0.96
13	350	7.5	60	<0.01
14	200	15	20	0.95
15	350	7.5	40	<0.01
16	350	7.5	40	<0.01
17	350	7.5	20	0.23
18	350	7.5	40	<0.01
19	350	7.5	40	<0.01
20	500	0	60	<0.01

4.7 Optimisation of critical variables

The specifications of the 3 runs carried out at the optimum conditions suggested by the model met all the LO10 specifications in terms of the ash content, viscosity at 40^{o}C, calorific value and flash point. The comparison can be viewed in table 4.8.

Table 4.8 Product, feed and LO10 specification comparison

Property	Used Lube Oil Properties	Final Product Properties	LO 10 Specifications
Ash content (wt%)	0.8 - 1.2	< 0.01%	< 0.08
Viscosity @ 40°C (cSt)	43 - 48	9.51	10
Flash point (°C)	75 - 90	>50	> 50
Calorific value (GJ/ton)	44	44	> 44

4.8 Limitations

The research does not include the longevity of full scale run times in terms of coking and or fouling in heat exchange equipment, namely the heating coil. Additionally the methodology used a common UALO feed for all experimentation and due to this, the model developed from the results may not be valid for other UALO feed stocks. Further work will have to be carried out on coking rates inside heat exchange equipment using random UALO feed stocks at the models predicted optimum running conditions in order to confirm the viability of the process at a production scale. It must also be carefully noted that the model is only valid for the variable ranges investigated.

4.9 Summary of answers to research questions

The literature review, experimentation, results and discussion revealed that the heat soak type visbreaker was a suitable process that is capable of breaking the additive package and substantially reducing the viscosity of UALO. The critical operating variables and their associated optimum values through literature, experimentation and modelling were confirmed to be temperature (475°C), pressure (15 bar) and residence time (60 min). The optimum operating variables produce an oil from UALO that meets all the required LO10 specifications at the required 90% yield.

5 Conclusion

This thesis set out to develop/identify the most efficient process that, from UALO, will produce a low viscosity, low ash and low sediment alternative to diesel and paraffin. The aim of the work was motivated by the lack of supply of profitable LO10 to the market. The thesis achieved the aim first by, qualitatively through literature understanding the properties of UALO, identifying the problems associated with its conversion to LO10, selecting a suitable process and identifying the critical operating variables. Secondly by quantitatively through experimentation and modelling, determines the effects that the critical operating variables had on the viscosity and yield. Also, the optimum critical operating variable values were identified.

The impurities (ash, additive package and asphaltenes) need to be broken/removed from the UALO, as well as its viscosity reduced from 48 cSt at 40^{o}C to 10 cSt at 40^{o}C, before UALO can be considered as LO10. The following sections summarise how this was achieved.

5.1 Qualitative

The study has identified through literature that thermal cracking via the free radical mechanism be the preferred process for producing low viscosity product LO10 from UALO (Green & Wittcoff, 2008). The free radical mechanism requires temperatures above 350^{o}C. In this temperature range, the additive package in UALO breaks down allowing for ash, soot and asphaltenes to drop out of suspension. The three most important requirements of thermal cracking are temperature, pressure and residence time (Sieli, 1998). The Heat soak type visbreaker was identified as the most suitable process to be used as a bench top test rig for experimentation in the quantitative part of the work.

5.2 Quantitative

The experimental results of this study revealed that all the three critical variables; i.e. temperature, pressure and residence time affected the viscosity. The constants in the quadratic model with the square root transformation revealed that temperature had the biggest effect on viscosity reduction with residence time having had the second biggest effect and pressure the third. Increasing any of the three variables results in a larger viscosity reduction, within the experimental range. The model developed, accurately predicted the optimum operating variable values (error < 5%) for the production of LO10 within specification. The optimum temperature, pressure and residence times were identified to be 475^{o}C, 15 bar and 60 min respectively. Lab tests confirmed that the additive package present in UALO completely breaks down at temperatures and residence times above 350^{o}C and 30 min respectively.

Ultimately the study has proven that at the pilot plant level, it is possible to produce LO10 from UALO with a heat soak type visbreaker, utilising the correct temperature, pressure and residence time following for the free radical thermal cracking mechanism to reduce the viscosity and break down the additive package.

5.3 Limitations

The research does not include longevity of full scale run times in terms of coking and or fouling in heat exchange equipment, namely the heating coil, and varying UALO feed stocks.

5.4 Recommendations

In order to ensure the successful development of a full scale heat soak type visbreaker that will feasibly convert UALO to LO10 for a Durban based oil refinery, the following needs to be carried out first. A full production scale pilot plant needs to be built; it will have to include all heat transfer equipment, most importantly the fired heater (heating coil) and the planned control philosophy. The heating coil design is an intricate part of the process in terms of heating and run length, but does not contribute significantly to the degree of cracking. Therefore a fired heater will need to be designed, paying close attention to correct flow

regimes, because incorrect flow regimes have been found to promote coking (Agorreta et al. 2011). The correct flow regimes will have to be identified through experimentation to ensure that there will be viable coking rates inside all heat exchange equipment at the models predicted optimum running conditions; temperature, pressure and residence time of 475^{o}C, 15 bar and 60 min respectively.

If the coking rates are found to be unacceptable, work will have to be carried out on reducing the asphaltene content of the feed, as grouping of asphaltenes at temperatures above 400^{o}C lead to cross linking and dehydration, yielding coke particles with radii of 1-5 μm. Grouping at lower temperatures result in precipitation on and fouling of furnaces and heat exchangers (Agorreta et al., 2011). Asphaltenes are therefore the biggest contributors to coke formation in heat exchange equipment with oil at high temperatures.

Varying feed UALO feed stocks will also have to be tested to determine flexibility and ultimately viability. Once the production scale pilot plant has been proven to be both functional and economically viable, the planning and construction of the full scale production plant can commence.

6 Bibliography

Abdel-Jabbar, M., Zubaidy, E. & Mehrvar, M., 2010, 'Waste Lubricating Oil Treatment by Adsorption Process Using Different Adsorbents', International Journal of Chemical and Biological Engineering, 3:2, p.70-72.

Agorreta, E., Angulo, C., Soriano, A., Font, C. & Respini, M., 2011, 'Simulation Model increases Visbreaker Conversion', Digitalrefining.com, Article1000425, p 2-5.

Ahmad I., Khan R., Ishaq M., Khan H., Ismail M., Gul K., Ahmad W., 2016, 'Valorization of spent lubricant engine oil via catalytic pyrolysis: Influence of barium-strontium ferrite on product distribution and composition' Journal of Analytical and Applied Pyrolysis, http://dx.doi.org/10.1016/j.jaap.2016.10.008, p 132-133.

Ahmed, N.S. & Nassar, A.M., 2011, 'Lubricating Oil Additives, Egyptian Petroleum Research Institute Egypt, DOI:10.5772/22923, P 249-265.

Angeira, C.S.M., 2008, 'Hydrocarbons Thermal Cracking Selectivity Depending on their Structure and Cracking Parameters', Prague, Institute of Chemical Technology Prague, 4-10.

Badger, M.W. & Harold, H., 2001, 'Viscosity Reduction in Extra Heavy Crude Oils', Pennsylvania, Pennsylvania State University, 16802-2303, p 461-462.

Bhaskar T., Uddin A., Muto A., Sakata Y., Omura Y., Kimura K., Kawakami Y., 2004, 'Recycling of waste lubricant oil into chemical feedstock or fuel oil over supported iron oxide catalyst', Fuel 83 (2004), P 10-11.

Luis C. Castaneda, José A.D. Munoz, Jorge Ancheyta, 2014, 'Current situation of emerging technologies for upgrading of heavy oils', Catalysis Today, http://dx.doi.org/10.1016/j.cattod.2013.05.016, p 250-256.

Catala, K.A., Karrs, M.S., Sieli, G., 2009, "Advances in delayed coking heat transfer equipment" Hydrocarbon Processing, p.45.

Clark, J., 2003, 'Cracking Alkanes', in chemguide, viewed 1 July 2016, from http://www.chemguide.co.uk/organicprops/alkanes/cracking.html

Corma A., Sauvanaud L., Mathieu Y., Al-Bogami S., Bourane A., Al-Ghrami M., 2017, 'Direct crude oil cracking for producing chemicals: Thermal cracking modeling', Fuel, http://dx.doi.org/10.1016/j.fuel.2017.09.099, p 726-727.

Faisal M., Gonzalez-Cortes S., Mohammed F., Tiancun X., Al-Megren H., Yang G.,Edwards P., 2018, 'Enhancing the production of light olefins from heavy crude oils: Turning challenges into opportunities' Catalysis Today, https://doi.org/10.1016/j.cattod.2018.02.018, p 5,8,9.

Goncharov D.V. & Belyaevskii M.Yu., 2005, 'Analysis and mathematical desciption of the thermal-oxidative cracking of naphtha', Chemical and Petroleum Engineering, vol.41, Nos. 3-4, p 193-195.

Green, M.M. & Wittcoff, H.A., 2006, 'Organic Chemistry Principles and Industrial Practice, How petroleum is converted into useful materials: Carbocations and free radicals are the keys', Wiley-VCH, ISBN: 978-3-527-30289-5, p 7.

Guichard B., Gaulier F., Barbier J., Corre T., Bonneau., Levitz P., Espinat D., 2017, 'Asphaltenes diffusion/adsorption through catalyst alumina supports-influence on catalytic activity' Catalysis Today, http://dx.doi.org/10.1016/j.cattod.2017.10.016, p 52.

Hosseini A., Zare E., Ayatollahi S., Vargas F., Chapman W., Kostarelos K., Taghikhani V., 2016, 'Electrokinetic behavior of asphaltene particles' Fuel, http://dx.doi.org/10.1016/j.fuel.2016.03.051, p 235-236.

Javanbakht G., Sedghi M., Welch W., Goual L., Hoepfner M., 2018, 'Molecular polydispersity improves prediction of asphaltene aggregation' Journal of Molecular Liquids, https://doi.org/10.1016/j.molliq.2018.02.051, p 383.

Khan R., Ahmad I., Khan H., Ismail M., Gul K., Yasin A., Ahmad W., 2016, 'Production of diesel-like fuel from spent engine oil by catalytic pyrolysis over natural magnetite' Journal of Analytical and Applied Pyrolysis, http://dx.doi.org/10.1016/j.jaap.2016.06.022, p 493-494.

King, G.E., 2009, 'Asphaltenes', viewed 22 July 2016, from http://GEKEngineering.com.

Komatsu, K., 2010, 'Catalytic Cracking of Paraffins on Zeolite Catalysts for the production of Light Oelifins', Tokyo, Department of Chemistry and Material Science, Tokyo Institute of Technology, p 1-2.

Kwaambwa, H.M., Goodwin, J.W., Hughes, R.W., & Reynolds, P.A., 2006, 'Viscosity Molecular Weight and Concentration Relationship at 298K of Low Molecular Weight cis-polyisoprene in a good Solvent', Gaborone, University of Botswana, p 14-15.

Lan X., Chnming X., Wang G. & Gao J., 2009, 'Reaction performance of FCC slurry catalytic cracking', Catalyst Today 140 (2009) 174–178, p 174-177.

Madelon F. Zady, 1999. 'Z-4: Mean, Standard Deviation, And Coefficient of Variation', viewed 15/12/2017, from https://www.westgard.com/lesson34.htm.

Medvedeva M.L., 1998, 'Possibilities of increasing the endurance and reliability of furnace coils in visbreaking and thermal cracking equipment', Chemical and Petroleum Engineering, vol.34, Nos. 7-8, p 451-452.

Mohaddecy, S., Sadighi, S., Ghabuli, O. & Rashidzadeh, M., 2011, 'Simulation of a visbreaking unit' Digitalrefining.com, Article1000396, p 1-2.

Mohammed R., Ibrahim I., Taha A., Mckay G., 2013, 'Waste lubricating oil treatment by extraction and adsorption' Chemical Engineering Journal, http://dx.doi.org/10.1016/j.cej.2012.12.076, p 346,348,349.

Nagiev A.G., Khalilov S.A., Guseinova & Nagiev G.A., 2016, 'Visualization of the factor of transported-catalyst density distrubution along the length of verticle pipelines in petroleum gas oil cracking units', Chemical and Petroleum Engineering, vol.52, Nos. 1-2. p16.

Nora Corporation, 2003, 'The Lowdown on Oil Breakdown, Machinery Lubrication', viewed 24 July 2016, from http://www.machinerylubrication.com/Read/475/oil-breakdown.

Osman D., Attia S., Taman., 2017, 'Recycling of used engine oil by different solvent' Egyptian Journal of Petroleum, http://dx.doi.org/10.1016/j.ejpe.2017.05.010, p 1-2.

Paridar S., Naza A., Karimi Y., 2018, 'Experimental evaluation of asphaltene dispersants performance using dynamic light scattering' Journal of Petroleum Science and Engineering, https://doi.org/10.1016/j.petrol.2018.01.013, p 570-572.

Rana S., Samano V., Ancheyta J., Diaz J., 2006, 'Current situation of emerging technologies for upgrading of heavy oils', Fuel 86 (2007), p 1219-1224.

Robinson, K.K., 2007, 'Reactor Engineering', St. Charles Illinois USA, Mega-Carbon Company, p1-2.

Rueda-Velasquez R., Gray M., 2017, 'A viscosity-conversion model for thermal cracking of heavy oils' Fuel, http://dx.doi.org/10.1016/j.fuel.2017.02.020, p 83-85.

Sadighi, S. & Moheddecy, S., 2013, 'Modeling of Thermal Oil Process in a Crude Oil Refinery', Iran, Journal of Petroleum and Gas Engineering, DOI 10.5897/JPGE2013.0151, p 81-82.

Shadman M., Dehaghani A., Badizad M., 2017, 'How much do you know about methods for determining onset of asphaltene precipitation', Petroleum, http://dx.doi.org/10.1016/j.petlm.2016.08.011, p 288-289.

Sharma, B.K., Bhagat, S.D., Erhan, S.Z., 2007, 'Maltenes and Asphaltenes of Petroleum Vacuum Residues: Physico-Chemical Characterization, Petroleum science and technology, ISSN: 1091-6466, p 93-97.

Shaw, D., 1992, 'Surface Activity and Micelle Formation', p1,3.

Sieli, G.M.,1998, 'Visbreaking the next generation' Foster wheeler publication', p1-4.

Sigma-Aldrich, 2018, 'Pressure-Temperature Nomogram Interactive Tool', https://www.sigmaaldrich.com/chemistry/solvents/learning-center/nomograph.html.

Sousa-Aguiar E.F., Trigueiro F.E. & Zanon Zotin F.M., 2013, 'The role of rare earth elements in zeolites and cracking catalysts', Catalyst today 218– 219 (2013) 115– 122, p 115-116.

Speight J.G., 2005, 'Petroleum: Chemistry, Refining, Fuels and Petrochemicals- Refining', Laramie, p 2.

Stratiev, D., Kirilov, K., Belchev, Z. & Petkov, 2008, 'How feed stocks affect visbreaker operations', Hydrocarbon processing, p105.

Wilczura-Wachnik, H., 2009, 'Catalytic Cracking of Hydrocarbons', Warsaw, University of Warsaw Faculty of Chemistry, p 2-7.

Zolotukhin V.A., 2004, 'New technology for refining of heavy crude and oil-refining resids', Chemical and Petroleum Engineering, vol.40, Nos. 9-10. p 585-587.

7 Appendix

7.1 Appendix A: Raw Results

Table 7.1 Raw Results

		Factor 1	Factor 2	Factor 3	Response 1					
Std	**Run #**	**A:Temperature**	**B:Pressure**	**C:Time**	**Viscosity (1)**	**Viscosity (2)**	**Viscosity (3)**	**Average**		
		Deg C	bar(g)	min	cSt	cSt	cSt	cSt	**Std dev**	**C of V (%)**
15	1	350	7.5	40	39.72	39.38	40.25	39.78	0.435384	1.09
12	2	350	15	40	38.13	37.94	38.61	38.23	0.33616	0.88
10	3	500	7.5	40	13.75	13.8	13.52	13.69	0.141067	1.03
11	4	350	0	40	40.24	40.89	41.39	40.84	0.304138	0.74
8	5	500	15	60	6.90	7.22	7.13	7.08	0.069469	0.98
5	6	200	0	60	50.62	51.02	50.86	50.83	0.100958	0.20
7	7	200	15	60	50.58	50.6	49.86	50.35	0.376081	0.75
18	8	350	7.5	40	39.51	39.99	38.94	39.48	0.525071	1.33
2	9	500	0	20	25.97	25.47	26.71	26.05	0.62043	2.38
9	10	200	7.5	40	51.43	52.31	50.45	51.40	0.93005	1.81
4	11	500	15	20	22.68	21.97	22.03	22.23	0.134261	0.60
1	12	200	0	20	52.88	53.48	53.88	53.41	0.252396	0.47
14	13	350	7.5	60	33.25	33.35	31.46	32.69	0.95889	2.93
3	14	200	15	20	52.61	52.1	52.53	52.41	0.222369	0.42
16	15	350	7.5	40	39.84	39.77	40.46	40.02	0.349036	0.87
19	16	350	7.5	40	39.49	38.92	38.89	39.10	0.113578	0.29
13	17	350	7.5	20	45.87	45.53	44.74	45.38	0.419563	0.92
17	18	350	7.5	40	39.34	39.83	40.37	39.85	0.307071	0.77
20	19	350	7.5	40	39.55	38.46	37.38	38.46	0.624503	1.62
6	20	500	0	60	7.63	7.5	8.04	7.72	0.271341	3.51
				Feed	55.67	55.71	55.49	55.62		

7.2 Appendix B: DOE Summary

Table 7.2 Design of Experiment Summary

File Version	**10.0.7.0**										
Design Wizard	**Optimization > Factorial / RSM > No HTC > All Numeric > 3 factors, 19 runs, goal design**										
Study Type	**Response Surface**		**Subtype**	**Randomized**							
Design Type	**Central Composite**		**Runs**	**20**							
Design Model	**Quadratic**		**Blocks**	**No Blocks**	**Build Time (ms)**		**15**				
Factor	**Name**	**Units**	**Type**	**Subtype**	**Minimum**	**Maximum**	**Coded**	**Values**	**Mean**	**Std. Dev.**	
A	Temperature	Deg C	Numeric	Continuous	200	500	-1.000=200	1.000=500	350	108.8214375	
B	Pressure	bar(g)	Numeric	Continuous	0	15	-1.000=0	1.000=15	7.5	5.441071876	
C	Residence T	min	Numeric	Continuous	20	60	-1.000=20	1.000=60	40	14.509525	
Response	Name	Units	Obs	Analysis	Minimum	Maximum	Mean	Std. Dev.	Ratio	Trans	Model
R1	Viscosity	cSt	20	Polynomial	7.08	53.41	36.45	14.24266	7.543785	Square Root	Quadratic

7.3 Appendix C: Results for drop test

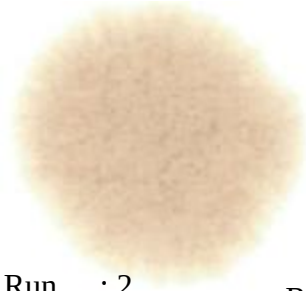

Run : 2
Temp : 350°C
Pres : 15 Bar
Time : 40 min

Run : 7
Temp : 200°C
Pres : 15 Bar
Time : 60 min

Run : 15
Temp : 350°C
Pres : 7.5 Bar
Time : 40 min

Run : 19
Temp : 350°C
Pres : 7.5 Bar
Time : 40 min

Run : 4
Temp : 350°C
Pres : 0 Bar
Time : 40 min

Run : 18
Temp : 350°C
Pres : 7.5 Bar
Time : 40 min

Run : 1
Temp : 350°C
Pres : 7.5 Bar
Time : 40 min

Run : 16
Temp : 350°C
Pres : 7.5 Bar
Time : 40 min

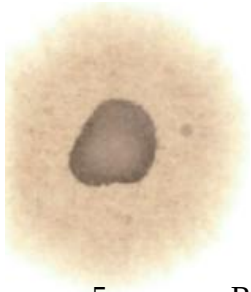

Run : 5
Temp : 500°C
Pres : 15 Bar
Time : 60 min

Run : 7
Temp : 200°C
Pres : 15 Bar
Time : 60 min

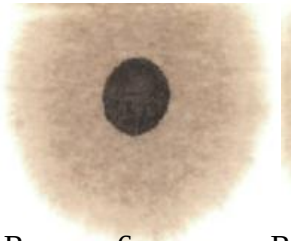

Run : 6
Temp : 200°C
Pres : 0 Bar
Time : 60 min

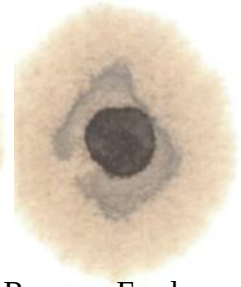

Run : Feed

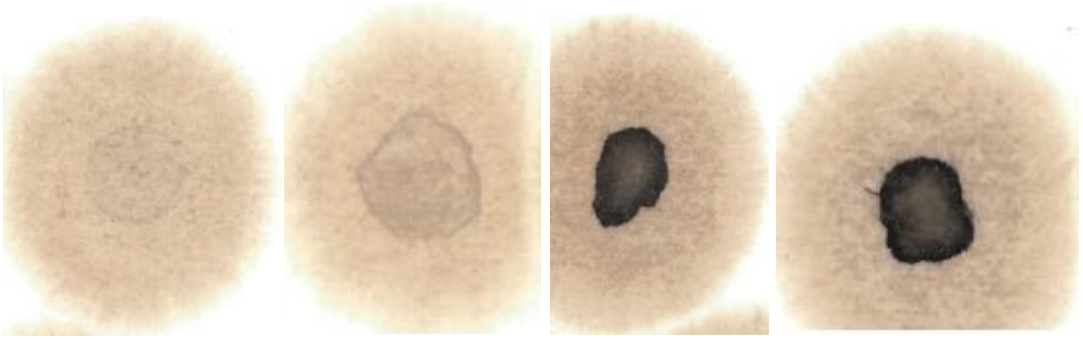

Run : 17	Run : 11	Run : 10	Run : 14
Temp : 350^{o}C	Temp : 500^{o}C	Temp : 200^{o}C	Temp : 200^{o}C
Pres : 7.5 Bar	Pres : 15 Bar	Pres : 7.5 Bar	Pres : 15 Bar
Time : 20 min	Time : 20 min	Time : 40 min	Time : 20 min

7.4 Appendix D: Pressure-temperature Nomogram

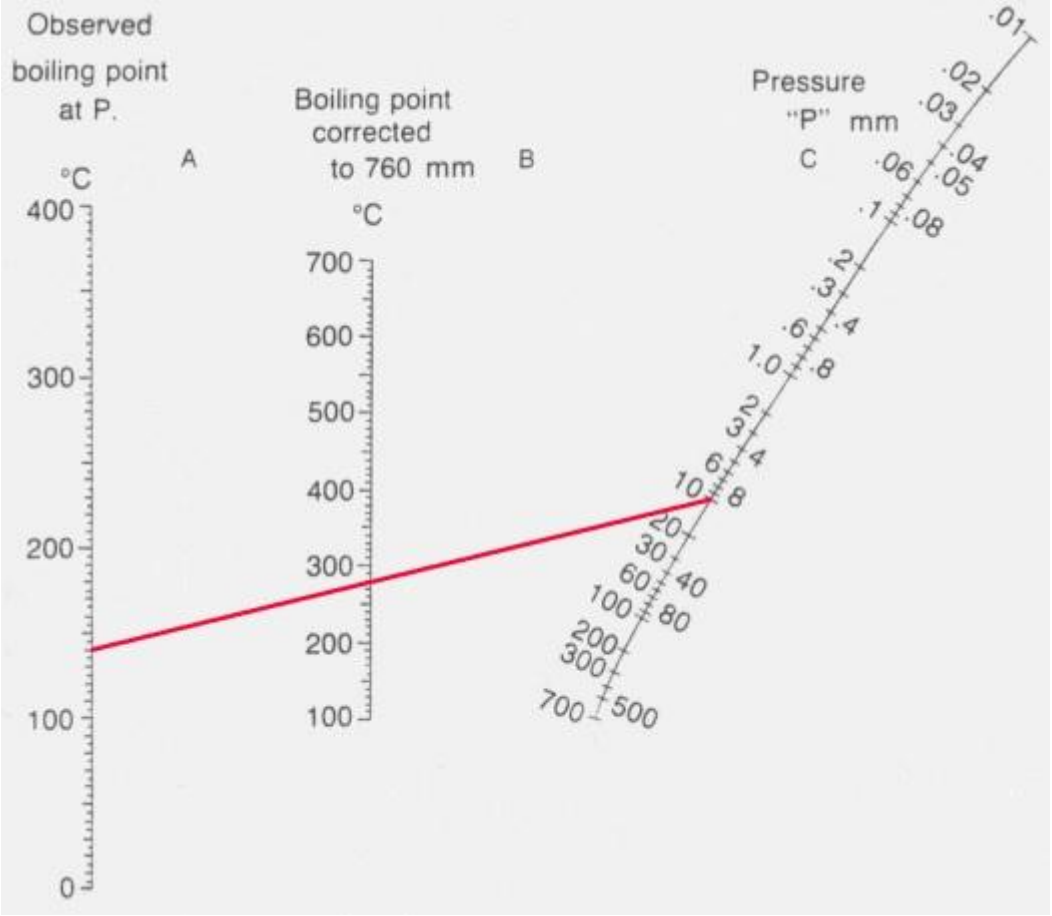

Figure 7.1 Pressure-temperature nomograph (adated from Sigma-Aldich, 2018)